JOURNAL OF PHYSIOLOGY AND PHARMACOLOGY 2020, 71, 6, 875-890
www.jpp.krakow.pl | DOI: 10.26402/jpp.2020.6.11

G.M. ALBADRANI[1], M.N. BINMOWYNA[2], M.N. BIN-JUMAH[1], G. EL-AKABAWY[3,4], H. ALDERA[5,6], A.M. AL-FARGA[7]

QUERCETIN PROTECTS AGAINST EXPERIMENTALLY-INDUCED MYOCARDIAL INFARCTION IN RATS BY AN ANTIOXIDANT POTENTIAL AND CONCOMITANT ACTIVATION OF SIGNAL TRANSDUCER AND ACTIVATOR OF TRANSCRIPTION 3

[1]Department of Biology, College of Science, Princess Nourah bint Abdulrahman University, Riyadh, Saudi Arabia;
[2]College of Applied Medical Sciences, Shaqra University, Shaqra, Saudi Arabia;
[3]Department of Basic Sciences, College of Medicine, Princess Nourah bint Abdulrahman University, Riyadh, Saudi Arabia;
[4]Department of Anatomy and Embryology, Faculty of Medicine, Menoufia University, Menoufia, Egypt;
[5]Basic Medical Sciences (Physiology Section), College of Medicine, King Saud bin Abdulaziz University for Health Sciences (KSAU-HS), Riyadh, Saudi Arabia; [6]King Abdullah International Medical Research Center (KAIMRC), Riyadh, Saudi Arabia;
[7]Department of Biochemistry, College of Sciences, University of Jeddah, Jeddah, Saudi Arabia

This study tested if the protective effect of quercetin (QUR) against experimentally-induced acute myocardial infarction (AMI) in rats involves modulating the Janus kinase 2/signal transducer and activator of transcription 3 (JAK2/STAT3) pathway. Rats were divided into 6 groups as sham-operated (control), control + QUR, AMI, AMI + QUR, AMI + S3I-210 (a STAT3 inhibitor), and AMI + QUR + S31-201. QUR (50 mg/kg/orally) and S3I-201 (a STAT3 inhibitor) (5 mg/kg/i.p.) were administered for 7 days before the induction of AMI and the experiment was ended 24 h post-AMI. Pre-treatment with QUR reduced the infarct size, improved the left ventricular (LV) functions and the structure of the myofibrils and the mitochondria, and reduced circulatory levels of lactate dehydrogenase (LDH), creatinine-kinase MB (CKMB), and troponin-I. QUR also reduced LV levels of reactive oxygen species (ROS) and malondialdehyde (MDA), inhibited the opening of the mitochondria transition pores (mtPTP), and reduced protein levels of cytochrome-C, cleaved caspase-3 and p-JAK2 (Tyr1007/1008) in the LVs of AMI rats. In the LV of both the control and AMI rats, QUR didn't affect the levels of p-JAK2 but significantly increased the levels of total glutathione (GSH) and manganese superoxide dismutase (MnSOD), reduced the levels of Bax and the nuclear levels and activity of NF-κB p65, tumor necrosis-factors-α (TNF-α), interleukin-6 (IL-6), and p-STAT1 (Ser727) but further increased the levels of p-STAT3 (Ser727). All these effects exerted by QUR were partially reversed but the decrease in nuclear protein levels and activity of NF-κB, levels of TNF-α and IL-6, and pSTAT3 were completely prevented by co-administration of S3I-201. In conclusion, QUR protects against MI by upregulation of antioxidants and activation of STAT3.

Key words: *quercetin, myocardial infarction, oxidative stress, inflammation, Janus kinase 2, signal transducer and activator of transcription 1, signal transducer and activator of transcription 3*

INTRODUCTION

Acute myocardial infarction (MI), driven by coronary artery occlusion, is a major worldwide cause of increased mortality and morbidity and one of the greatest socioeconomic burdens to society, patients, and the countries healthcare systems (1). As a consequence of MI, cardiomyocytes death deteriorates the contractile function of the heart which eventually leads to the development of irreversible heart failure (HF) (1). Currently, a surge of evidence has confirmed that oxidative stress and inflammation are two-interconnected mechanisms that initiate cardiomyocyte apoptosis in the infarct area during an acute MI by activating different signaling pathways (2, 3).

The emerging roles of the Janus kinase/signal transducer and activator of transcription (JAK/STAT) signaling pathway in regulating cardiomyocytes health and cardiac function post-cardiac ischemia have been established (4, 5). In general, the JAK/STAT pathway, a gp130/dependent pathway, is a stress-response pathway that regulates numerous biological activities including cell proliferation, differentiation, immunity, inflammation, and apoptosis (4-6). In the neonatal and adult heart, all JAK/STAT members (JAK1, JAK 2, JAK3, STAT1-4, STAT5a, STAT5b, and STAT6 are abundantly expressed in many cardiac resident cells such as the myocytes, endothelial cells, and fibroblasts (7, 8). All members of the JAK/STAT pathway are activated in the ischemic heart/cardiomyocytes and remain significantly high up to 1 week (4, 5, 9, 10). During cardiac ischemia, the most studies members are JAK2, STAT1, STAT3 were a mechanical stretch, pressure overload, and overproduction of angiotensin II (ANG II), reactive oxygen species (ROS), and inflammatory cytokines (i.e. IL-6) are the best-known inducers (11, 12).

In the heart as well as other tissues, the cellular effects STAT1 and STAT3 are contradictory. During AMI, STAT1 is always an apoptotic signal that induces the transcription of many apoptotic genes including caspase-1, Fas, FasL, p53, and Bax, and apoptotic autophagy (13-16). However, the activation of STAT3 is a protective mechanism during ischemia pre-conditioning and in the ischemic hearts and is associated with antioxidant, anti-inflammatory, and anti-apoptotic effects (16-18). Indeed, STAT3 can preserve the mitochondria integrity and cellular respiration, reduce mitochondria generation of ROS, maintain microtubules structure, suppress the nuclear factor-kappaB (NF-κB), stimulate the expression of anti-oxidant and anti-apoptotic genes, induce protective autophagy, and control the deposition of the extracellular matrix (EXM) (19).

On the other hand, plant flavonoids were shown to exert numerous cardioprotective effects (20). Quercetin (QUR) a subclass of flavonoids is one of the most abundant flavonoids in fruits, citrus, berries and cherries, onions and broccoli, and beverages such as red wine and tea (21). Currently available data have shown an important medicinal value of QUR in a variety of conditions due to its potent antioxidant, anti-inflammatory, and anti-apoptotic potential, as well as its ability to modulate various signal transduction pathways (21). In several animal models of cardiac I/R injury and MI, QUR was shown to be an effective therapy that can reduce the infarction size and preserved cardiovascular function (22-26). Also, but *in vitro*, QUR prevented cardiomyocyte death after exposure to I/R episode or exposure to H_2O_2 (27). Also, QUR has independent anti-apoptotic effect mediated by downregulating p53 and Bax and upregulation of Bcl2 (28). In all these studies, the beneficial effects of QUR as attributed to suppressing the generation of ROS, inhibition of the angiotensin-converting enzyme (ACE), and NF-κB activities, and improving endothelium vascular relaxation. Of note, QUR potentiates the anti-proliferative effect of interferon-α in hepatocellular carcinoma cells by activating the JAK/STAT pathway signaling (29). In the same line, QUR and its metabolite isorhamnetin increased GLUT-4 translocation and promoted glucose uptake in myotubes, at least, through activating JAK/STAT3 but not the STAT1 pathway (30). On the contrary, QUR prevented cultured cardiomyocyte death by reducing the activity of Src kinase/38MAPK/STAT3 (27).

However, much is still unknown about the precise mechanism(s) that underlie(s) the protective effect of QUR against MI. As discussed above, and given the important role of STAT1/3 in modulating cardiac redox status, inflammation, and apoptotic, it was of interest for us to investigate if the previously reported cardioprotective effect of QUR in MI animals models involves modulating the JAK/STAT pathway. This mechanism was never tested in any animal models of cardiac I/R injury or MI after treatment with QUR. Therefore, in this *in vivo* rats' study, we are presenting the first evidence in the literature that pre-administration of dietary QUR protects against AMI mainly by independent mechanisms, namely upregulation of antioxidant and activation of STAT3.

MATERIALS AND METHODS

Animals

Adult male Wistar albino rats (220 ± 10 g) were supplied from the animal center of the College of Pharmacy at King Saud University (Riyadh, Saudi Arabia). The animals were bred and housed in standard conditions (temperature 22 ± 1°C, humidity 55 – 60%). During the experimental period, all animals were fed a normal diet and had free *ad libitum* access to water.

All animal experiments including treatment, surgery, blood, and tissue collection were following and approved by the Institutional Review Board (IRB. No: 20-0177), Princess Nourah Bint Abdul Rahman University, Riyadh, Saudi Arabia.

Induction of acute myocardial infarction

Acute myocardial infarction (AMI) was introduced to rats as previously performed by others (31). In brief, all rats were anesthetized by intraperitoneal (i.p.) injection of a 1% solution of sodium pentobarbital (60 mg/kg). Once anesthesia was confirmed and all rats were ventilated artificially on a heating pad. The electrocardiogram (ECG, lead II), heart rate, and respiratory rate were continuously monitored using a PowerLab data acquisition system (Model ML780, ADInstruments, Bella Vista, Australia) and associated software (LabChart 8). Then, the chest was opened at the levels of the 4th intercostals, the heart was exposed, the pericardium was removed, and the left anterior descending (LAD) artery was allocated. The LAD was permanently tied at a location between the pulmonary cone and the left atrial appendage, using an 8/0 suture. Once MI was confirmed by the ST elevation, the muscles and chest were closed (5/0 sutures) and the thorax was empty from the air using a syringe. For all animals, intramuscular (i.m.) penicillin and subcutaneous (s.c.) buprenorphine (0.1 mg/kg) was then administered to prevent post-operative infection and pain. The rats were returned to their cages and used directly in the experimental procedure as shown below.

Drugs preparation

Quercetin (QUR) (Cat. NO. Q4951) and S3I-201 (a STAT3 phosphorylation inhibitor) (Cat. No. S1155) were purchased from Sigma Aldrich, St. Louis, MO, USA. QUR was always dissolved freshly in 1% dimethyl sulfoxide (DMSO)/phosphate-buffered saline (PBS) solution to a final working solution of 10 mg/ml. On the other hand, S3I-201 was dissolved in 100% DMSO and then diluted with corn oil to 1%. Briefly, 22 mg of S3I-201 was dissolved in 200 µL DMSO to give a master liquid concentration of 110 mg/ml. Then, 200 µl of this DMSO master liquid was mixed with 19800 µL corn oil to give a working solution of 1.1 mg/ml. The vehicle for this part was prepared by dissolving 200 µl of 100% DMSO in 19800 µL corn oil (1% DMSO). The final concentration of DMSO in these preparations was 1%.

Experimental design

Control and survival rats were divided into 5 groups (n = 12/group) as follows:

1) a control sham-operated group: received equivalent volumes of the vehicles (1% DMSO orally, and 1% DMSO (in corn oil) (i.p.) for 7 days and then exposed to sham surgery without tying the LAD;

2) a QUR-control sham-operated group: received QUR solution (50 mg/kg, daily, orally) for 7 days and then exposed to sham surgery as in the sham group,

3) an AMI model group: pre-treated with equivalent volumes of the vehicles (1% DMSO orally, and 1% DMSO (in corn oil) (i.p.) for 7 days daily and then exposed to AMI as described in the methods;

4) AMI + S3I-201-treated group: were pre-treated with S3I-201 solution (5 mg/kg, i.p.) once every 2 days for 7 days, and then exposed to AMI;

5) QUR + AMI-treated group: pre-treated with QUR solution (50 mg/kg, daily, orally) for 7 days and then expose to AMI;

6) QUR + S3I-201 + AMI-treated group: were co-treated with QUR and S3I-201, at the same doses and routs of administration as in the previous groups and then exposed to

AMI. In the latter group, S3I-201 was initially given on the first treatment day 1 h before the administration of QUR.

The experiment was ended 24 h after induction of MI (or the sham surgery in other groups). The dose and route of administration of QUR that was selected in this study were adopted from previous studies which have shown a cardioprotective effect in animal models of AMI and I/R injury and was confirmed in our preliminary data (32, 33). The dose and route of administration of S3I-201 were adopted from similar *in vivo* studies in rats to prevent the cardiac activation of STAT3 (34, 35). In our preliminary data, we have noticed that individual or combined administration of oral 1% DMSO (orally) and/or 1% DMSO (in corn oil) has no effects on cardiac structure and function. For this reason, oral administration of an equivalent volume of 1% DMSO and i.p. administration of an equivalent volume of 1% DMSO (in corn oil) were used as a vehicle.

Left ventricle hemodynamic measurements

Twenty-four hours post-infarction, cardiac hemodynamic measurements were assessed in all groups of rats. In brief, rats were anesthetized with a 1% solution of sodium pentobarbital (50 mg/kg; i.p.). The carotid artery was allocated and freed from the surrounding tissues and nerves. An SPR-320 pressure Millar catheter was directly inserted into the carotid artery and forwarded into the LV to acquire the pressure signal on a PowerLab data acquisition system (Model ML780, ADInstruments, Bella Vista, Australia). The recording of the pressure signal was continued for 20 min. The signal obtained during the last 10 min was used to derive all hemodynamic parameters using the LabChart 8 software (ADInstruments, Bella Vista, Australia). The calculated parameters were LV systolic pressure (LVSP), LV end-diastolic pressure (LVEDP), maximal rate of rising in LV pressure (+dP/dt), and maximal rate of decline in LV pressure (–dP/dt). This procedure was done for 8 randomly selected rats.

Serum and tissue collection

Directly after the left LV hemodynamics measurement, the chest of each rat was opened and a blood sample (1 ml/each) was collected directly from the right atrium into a plain tube. The blood tubes were allowed to sit for 30 min and then centrifuged at 1500 × g for 10 min to separate the sera. All sera samples were stored at –20°C and used later for the measurement of some cardiac markers. Then, the animals were killed by cervical dislocation and their hearts were rapidly excised on ice. Hearts from 6 rats/group were frozen at –20°C for 10 min and then used for the determination of infarct size as described below. The area of the maximum infarction of each LV (pale area) of the remaining hearts was isolated and cut into small pieces, some of which were fixed in 10% formalin for histological evaluation, fixed in 2.5% glutaraldehyde buffer for electron microscopy studies, or snap-frozen in liquid nitrogen, and stored at –80°C for further biochemical and molecular studies.

Determination of the infarct size

This has been done as previously described by others (36, 37). In brief, the frozen hearts were sliced horizontally into 6 – 8 slices from base to apex (2 – 4 mm sections) using a razor blade on cold surface slices. The slices were used were stained with 1% 2, 3, 5-triphenyl-tetrazolium chloride (TTC) (Cat. No. T8877, Sigma-Aldrich, St. Louis, Missouri, USA) for 5 min at 37°C. Then, the slices were fixed with 4% formaldehyde for 12 h at room temperature. Using this protocol, the viable tissue stained red and dead tissue remains unstained. All slides were examined using a Nikon Eclipse E800 microscope using a 1 × objective and all photographs were captured using the associated camera (model Retiga CCD camera and the associated software (Openlab, Santa Cruz, CA, USA). All images were then analyzed manually using the online ImageJ online software. In the analysis, we have traced the areas of the infarcted region and the total LV of each image which was reflected by the software. The infarction size was calculated by the sum of the infarct area of all sections over the sum of the total area of LV of all section X 100.

Biochemical analysis in the serum and the left ventricles

Serum levels of troponin-I and creatinine kinase-MB (CKMB) were measured from all collected blood samples (n = 12) using a special ELISA kit for rats (Cat. No. E4737 and Cat. NO. E4608, BioVision, Milpitas, CA, USA).

Biochemical analysis of the left ventricles

LV homogenates for the biochemical parameters were prepared by homogenizing the infarcted tissue with 9 volumes an ice-cold phosphate buffer saline (PBS/pH = 7.4) (Cat. No. 20012043, Thermo Fisher Scientific, Waltham, MA, USA) plus 10-µL protease inhibitor cocktail (Cat. No A32965, ThermoFisher Scientific Waltham, MA, USA). The nuclear-cytoplasmic/nuclear extracts were prepared using a commercially available kit (Cat. NO. 78833, ThermoFisher Scientific). Total levels of reduced glutathione (GSH) were measured using an assay kit (Cat. No. K454 (BioVision, Milpitas, CA, USA). Levels of interleukin-6 (IL-6) were measured using an ELISA kit (Cat. No. K4145, BioVision, Milpitas, CA, USA). Levels of superoxide dismutase (SOD) were measured using a rat's assay kit (Cat. No. E458, BioVision, Milpitas, CA, USA). Levels of tumor necrosis factor-alpha (TNF-α) were determined by an ELISA kit (Cat. No., K1052, BioVision, Milpitas, CA, USA). Levels of malondialdehyde (MDA) were determined using an assay kit (Cat. No. K454, BioVision, Milpitas, CA, USA). ROS levels were measured using a special fluorometric kit (Cat. No. E-BC-K138-F, Elabscience, Houston, TX, USA USA). The activity of NF-κB p65 was determined using a specific assay kit (Cat. No. 31102, Active Motif, Tokyo, Japan). The absorbance and fluorescence signals in all analyses were measured by the M2 Spectramax plate reader (Molecular Devices, San Jose, CA, USA) and (FL600Bio fluorescent reader (Tek Instruments, Inc., Winooski, VT, USA), respectively. All analyses/kits were conducted for 6 samples/group, per the manufacturer's instructions.

Measurements of mitochondrial permeability transition pore (mtPTP)

The isolation of the mitochondria from frozen infarcted LVs was performed using a commercially available mitochondria isolation kit (Cat. No. Ab110168, Abcam, Cambridge, UK) and per the manufacturer's instructions. The purity of the isolated mitochondria was confirmed by Western blotting using a VDAC (a mitochondrial-specific protein) antibody (Cat. No. 4688, Cell Signalling Technology, Danvers, MA, USA). The mitochondria mtPTP was determined according to the methods described by others (38-41). According to this protocol, treating the mitochondria with $CaCl_2$ or ROS generating agent (*i.e.* tert-butyl hydroperoxide, *t*-BuOOH) causes mitochondria swelling and rupture which leads to a decrease in the absorbance overtime at 540 nm. Accordingly, two parameters can be calculated 1) the V_{max} (the time maximum rate of the decrease in the absorbance per min and 2) time to reach V_{max}. Briefly, the isolated fresh mitochondria were suspended in 0.5 ml buffer containing 215 mM mannitol, 71 mM sucrose, 3 mM HEPES, 5 mM succinate to a final concentration of 1 mg/ml. These isolated mitochondria were then

individually treated with 400 µM $CaCl_2$ in conjugation with 75 µM t-BuOOH and the decrease in absorbance was monitored for 10 min at 540 nm. mtPTP was measured for n = 6 samples/group.

Western blotting

Frozen infarcted tissue was homogenized in 9 volumes 1X RIPA buffer (Cat No. 156034, Abcam, Cambridge, UK). The resulted supernatants were isolated after centrifugation at 4°C for 10 min at 11000 × g. All proteins were determined in total cell homogenates except NF-κB and cytochrome-C, which were determined in the pre-isolated nuclear and cytoplasmic fractions. All samples were prepared in the SDS-PAGE loading buffer (Cat. No. MBS176755, MyBioSource, San Diego, CA, USA) and boiled for 5 min. Equal proteins from each sample (40 µg) were loaded in an 8 – 12% SDS page and separated by electrophoresis. The samples were then transferred into on nitrocellulose membranes, blocked with skimmed milk, washed (3x/5 min), and then blotted with the primary antibodies against cleaved caspase-3 (Asp175) (Cat. No. 9664, 17:19 kDa), Bax (Cat. No. 2744, 20 kDa, 1:1000), cytochrome-C (Cat. No. 11940, 14 kDa, 1:1000), JAK2 (Cat. No. 3230, 125 kDa, 1:1000), p-JAK2 ($Tyr^{1007/1008}$) (Cat. No. 3771, 125 kDa), STAT3 (Cat. No. 9139, 79/86 kDa, 1:1000), p-STAT3 (Ser^{727}) (Cat. No. 49081; 86 kDa, 1:500), STAT 1 (Cat. No. 14994,84/91 kDa), p-STAT1 (Tyr^{727}) (Cat. No. 9177, 91 kDa, 1:500), NF-κB p65 Antibody (Cat. No. 3034, 65 kDa, 1:1000), lamin A/C (Cat. No. 4777, 63/74 kDa, 1:2000), and β-actin (Cat. No. 4970, 45 kDa) (Cell Signalling Technology, Danvers, MA, USA). Membranes were then washed again and incubated with the corresponding 2nd antibodies (1:1000). The incubation with the 1st and 2nd antibodies was done at room temperature for 2 h with continuous shaking. Washing between steps and preparation of the skimmed milk and antibodies were done in tris-buffered saline (TBS)-tween 20 (TBST) buffer. Membranes were stripped up to 3 times, in which the phosphorylated proteins were detected first. Bands were visualized using a price ECL substrate (Cat. No. 32109, ThermoFisher Scientific, Waltham, MA, USA). All bands were scanned and analyzed using the LI-COR C-DiGit scanner (Lincoln, NE, USA). Normalization between the stripped gels was done using an internally known sample. Values are presented for n = 5 samples/group.

Histological evaluation

For morphological analysis, parts of the freshly isolated LVs (n = 5/group) of all groups were first fixed in 10% buffered formalin for 20 h. Next, the fixed tissues were dehydrated in ethanol (70 – 100%), cleared in xylene, and embedded in paraffin wax. Then, all tissues were sectioned at a thickness of 5 µM, routinely stained with hematoxylin and eosin, and examined under a light microscope (Nikon Eclipse, model ME600, Spectrographic Ltd, Leeds, UK). For the TEM, small parts of the LVs (n = 3 rats/group) were fixed for 24 h in glutaraldehyde solution and then fixed in cacodylate buffer containing 1% osmium tetraoxide (1%). The tissues were then dehydrated in ethanol and embedded in Spurr's resin. Finally, all LVs parts were stained with uranyl acetate and lead citrate stains and examined under the transmission electron microscope

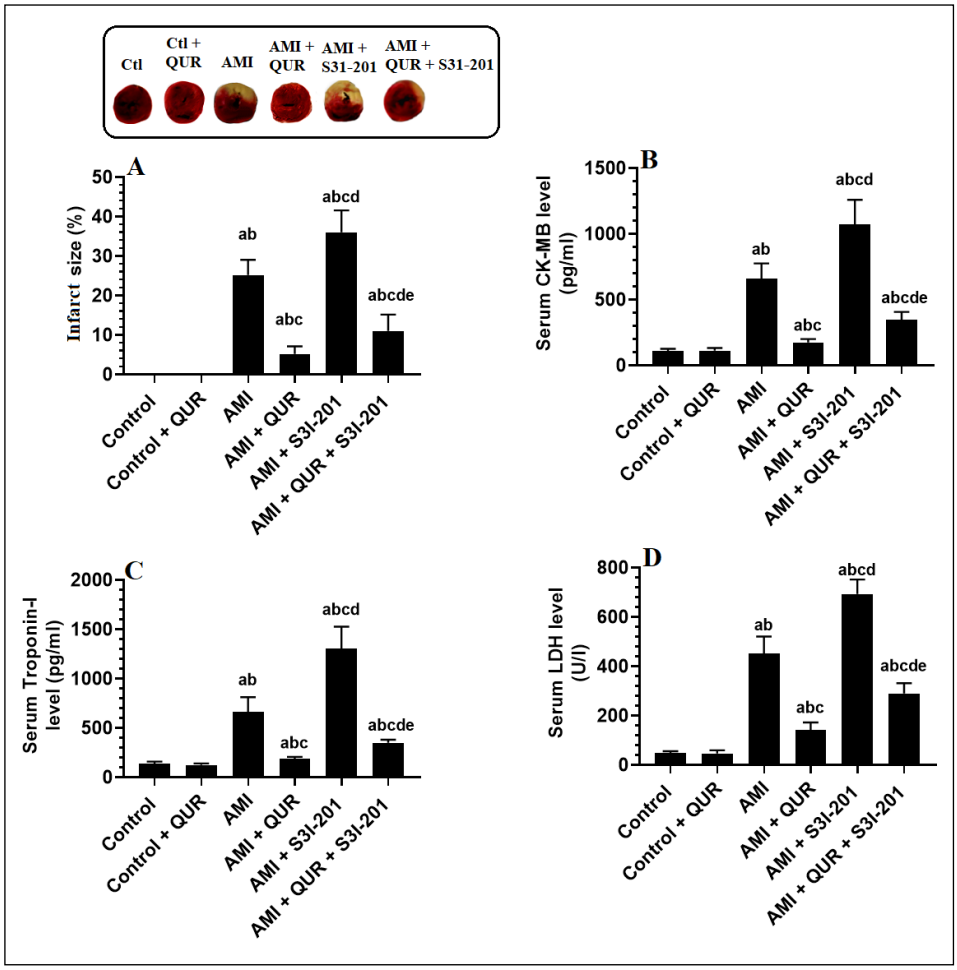

Fig. 1. Infarct size and serum levels of creatinine kinase (CK-MB), troponin-I, and lactate dehydrogenase (LDH) in all groups of rats. All data were analyzed by 1-way ANOVA followed by Tukey's *t*-test. And the degree of significance was considered at $P < 0.05$. Data are presented as mean ± SD of n = 6/group. [a]: significantly different as compared to the control group; [b]: significantly different as compared to control + quercetin (QUR). [c]: significantly different as compared to acute myocardial infarction (AMI)-induced rats. [d]: significantly different as compared to AMI + QUR. [e]: significantly different as compared to MI + S31-201 (a stat inhibitor).

(TEM) (model HF3300, Hitachi). All mages were examined by an external observer.

Statistical analysis

GraphPad Prism statistical software (V8) (San Diego, CA, USA) was used for statistical analyses. Normality was tested using the Shapiro-Wilk test. All analyses were conducted using one-way analysis of variance (ANOVA 1) followed by Tukey's *post hoc* t-test. The values were presented as mean ± standard deviation (SD) and were considered significantly different ta $P < 0.05$.

RESULTS

Quercetin reduces infarct size and preserves cardiac function partially in a STAT-3-dependent manner

Normal LV appearance with normal levels of circulatory cardiac markers were seen in the control + QUR-sham-operated rats as compared to control sham-operated rats (*Figs*. *1A-1D*, *2A* and *2B*, *3A* and *3B*). AMI-induced rats showed a large infarction in their LVs (25.1 + 3.9%) and significantly higher serum levels of cardiac injury markers including CK-MB, troponin-I, and LDH as compared to control rats (*Fig*. *1A-1D*). Besides, they showed significantly higher levels of LVEDP and decreased the value of LVSP and the maximum increase or decrease in dp/dt (dp/dt_{max} and dp/dt_{min}, respectively) as compared to control rats (*Fig*. *2A-2D*). On the contrary, administration of QUR to AMI-induced rats (AMI + QUR) significantly lowered the infarct area (5.1 ± 1.9%), circulatory levels of CK-MB, LDH, and troponin-I, and values of LVEDP but significantly increased values of LVSP, $dp/dt_{max,}$ and dp/dt_{min} as compared to AMI-induced rats (*Figs*. *1A-1D* and *2A-2D*). The levels of all these markers as well as the infarct area remained significantly higher than their corresponding levels seen in the sham or QUR control rats (*Figs*. *1A-1D* and *2A-2D*). However, AMI + S31-201 showed significantly higher infarct area (376 ± 5.5%) and higher circulatory levels of CK-MB, LDH, and troponin-I, as well values of LVEDP with a concomitant significant decrease in the values of LVSP as compared to AMI-induced rats (*Figs*. *1A-1D* and *2A-2D*). The alterations of all these parameters were the maximum in this group of rats as compared to all other groups (*Figs*. *1A-1D* and *2A-2D*). On the other hand, a significant reduction in the infarct area (11.7 ± 4.1%) with a parallel reduction in the circulatory levels of CK-MB, LDH, and troponin-I, and values of LVEDP with a significant increase in the values of LVSP, $dp/d_{tmax,}$ and dp/dt_{min} were observed in AMI + S31-201 + QUR as compared to AMI-induced rats and AMI + S31-201-treated rats (*Figs*. *1A-1D* and *2A-2D*). However, the levels of all these parameters remained significantly varied as compared to those seen in the AMI + QUR-treated rats (*Figs*. *1A-1D* and *2A-2D*).

Quercetin improves infarcted left ventricles structure partially in a STAT-3-dependent manner

Changes in histopathology of LVs of all experimental groups of rats are shown in *Fig*. *3A-3F*. Normal cardiac structure with intact myofibrils and intercalated disk and oval centrally located nuclei were observed in the control sham and control + QUR sham-operated rats (*Fig*. *3A* and *3B*). However, cardiomyocyte damage (rupture) with disorganized myofibrils (wavy forms), vacuolization, and loss of cardiomyocyte nuclei

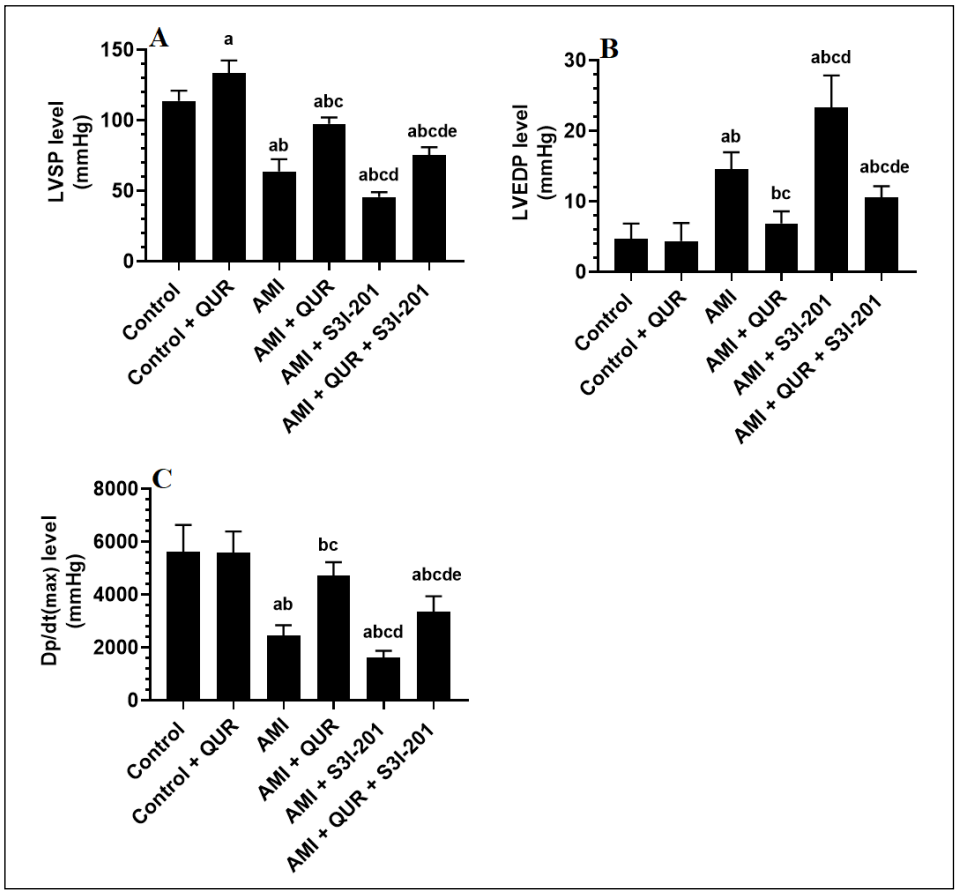

Fig. *2*. Cardiac hemodynamic parameters in the left ventricles of all groups of rats. All data were analyzed by one-way ANOVA followed by Tukey's *t*-test. And the degree of significance was considered at $P < 0.05$. Data are presented as mean ± SD of n = 6/group. [a]: significantly different as compared to the control group; [b]: significantly different as compared to control + quercetin (QUR). [c]: significantly different as compared to acute myocardial infarction (AMI)-induced rats. [d]: significantly different as compared to AMI + QUR. [e]: significantly different as compared to MI + S31-201 (a STAT3 inhibitor).

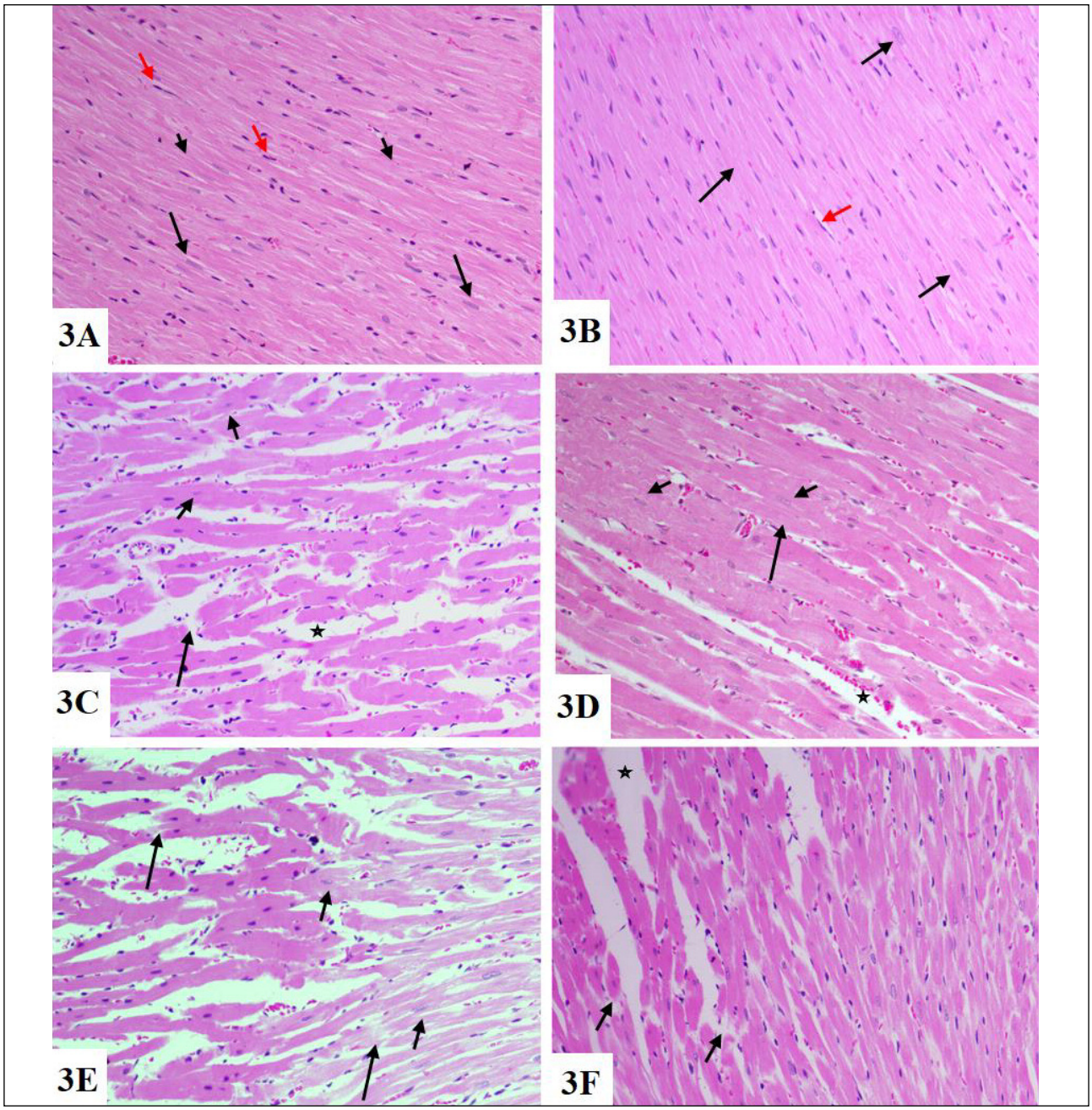

Fig. 3. Histological evaluation of the changes in the left ventricles of all groups of rats after staining with haematoxylin and eosin. (*A*) and (*B*): were taken from control sham and control + quercetin- (QUR)-sham operated rats and showed normal cardia myofibrils structure that runs horizontally with intact centrally located nuclei (long arrow), peripheral endothelial cells (red arrow), and intact intercalated disk (short arrow). (*C*): was taken from a rat with an acute myocardial infarction (AMI) and showed the dominancy of the way forms of the myofibrils, damaged myofibrils (short arrow), increased spaces between the myofibrils (star), and damaged nuclei (short arrow). (*D*): was taken from an AMI + QUR-treated rats and showed an almost normal appearance of the cardiomyocytes myofibrils that looks similar to those observed in the control of sham-operated rats. However, a few damages still exist. (*E*): was taken for an AMI + IS31-201-treated rat and showed severe rupture in the cardiomyocytes myofibrils (long arrow) and intercalated disks (short arrow) with disorganized nuclei. (*F*): was taken from an AMI + QUR + IS31-201-treated rat and showed improvement in the structure of the myofibrils. However, the wavy form of myofibrils, few vacuoles, and disorganized nuclei are still seen in this group of rats. × 200.

were observed in AMI-induced rats as compared to control rats (*Fig. 3C*). On the other hand, almost normal cardiomyocyte structure with intact myofibrils and intercalated disks and decreased spaces between the myofibrils with the presence of less damage was observed in the LVs of AMI + QUR-treated rats (*Fig. 3D*). The histological features obtained from AMI + S31-201-treated rats revealed more severe rupture in the cardiomyocytes structure with disorganized nuclei and damaged intercalated disks as compared to all other groups (*Fig. 3E*). However, LVs obtained from AMI + S31-201-treated rats showed improvement in the structure and organization of the myofibrils as compared to AMI and AMI + S31-201-treated rats with the presence of wavy forms of myofibrils, disorganized nuclei, and some vacuoles (*Fig. 3F*).

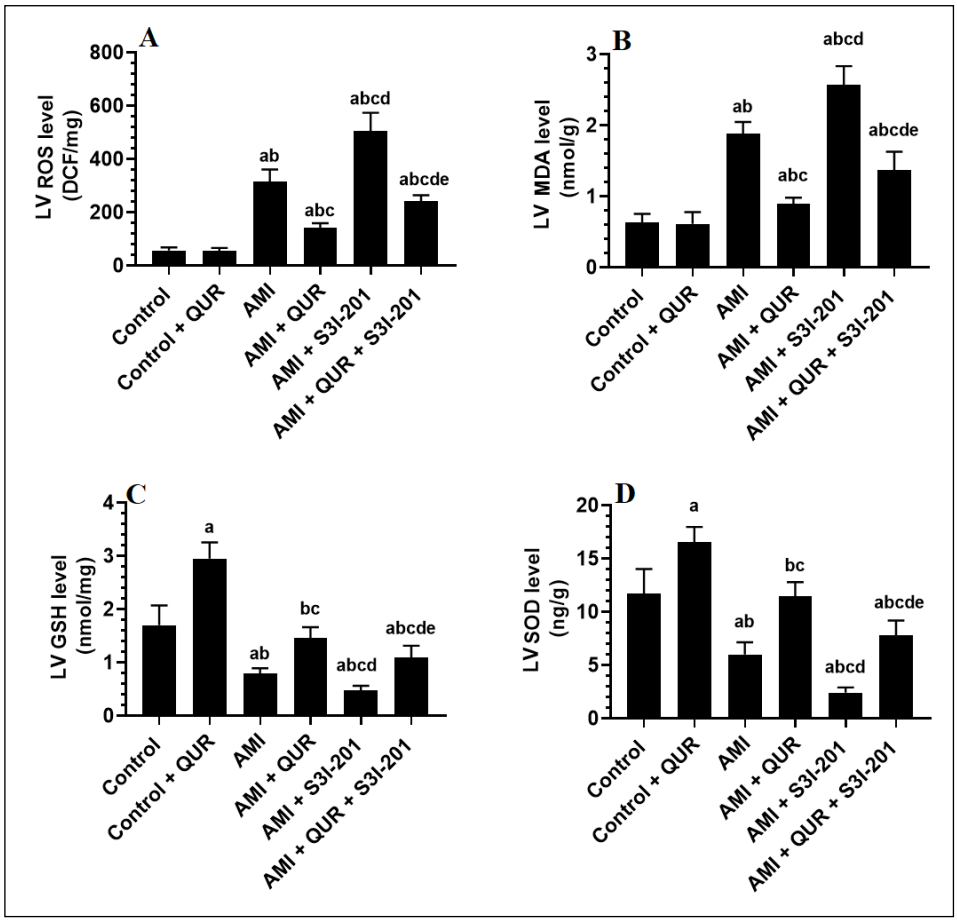

Fig. 4. Levels of reactive oxygen species, malondialdehyde (MDA), total glutathione (GSH), and superoxide dismutase (SOD) in the left ventricles of all groups of rats. All data were analyzed by one-way ANOVA followed by Tukey's *t*-test. And the degree of significance was considered at $P < 0.05$. Data are presented as mean ± SD of n = 6/group. [a]: significantly different as compared to the control group; [b]: significantly different as compared to control + quercetin (QUR); [c]: significantly different as compared to acute myocardial infarction (AMI)-induced rats; [d]: significantly different as compared to AMI + QUR; [e]: significantly different as compared to MI + S31-201 (a stat inhibitor).

Quercetin suppresses the generation of reactive oxygen species and lipid peroxidation but increases antioxidant levels in the infarcted myocardium, partially in STAT3-dependent manner

While levels of ROS and MDA were not significantly altered, levels of GSH and SOD were significantly increased in the LVs of QUR-treated sham-operated rats as compared to control sham-operated rats administered the vehicle (*Fig. 4A-4D*). The levels of ROS and MDA were significantly increased while the levels of GSH and SOD were significantly decreased in the infarcted LVs of AMI-induced rats as compared to those observed in the sham-operated control rats (*Fig. 4A-4D*). A significant reduction in the levels of ROS and MDA with a concomitant significant increase in the levels of GSH and SOD were depicted in the infarcted LVs of the AMI + QUR-treated rats as compared to AMI-induced rats (*Fig. 4A-4D*). Although the levels of ROS and MDA remained significantly higher, the LV levels of GSH and SOD were not significantly varied between sham-operated control rats and AMI + QUR-treated rats (*Fig. 4A-4D*). On the other hand, significantly higher levels of ROS and MDA and lower levels of GSH and SOD were seen in the infarcted LVs obtained from AMI + S3I-201 as compared to AMI-induced rats (*Fig. 4A-4D*). The maximum increase in ROS and MDA and the maximum decrease in the levels of GSH and SOD were observed in this group of rats (*Fig. 4A-4D*). On the opposite, levels of ROS and MDA were significantly decreased and levels of GSH and SOD were significantly increased in AMI + QUR + S3I-201 as compared to AMI and AMI + S3I-201-treated rats (*Fig. 4A-4D*). However, the LV levels of ROS and MDA remained significantly higher and levels of GSH and SOD remained significantly lower than their corresponding levels observed in either the control or QUR-sham operated rats (*Fig. 4A-4D*).

Quercetin suppresses nuclear factor-κB and inflammatory cytokines release in a STAT3 dependent manner

Levels of TNF-α, IL-6, and nuclear activity of NF-κB, as well nuclear protein level of NF-κB were significantly decreased in the infarcted LVs of the control + QUR sham-operated rats but significantly increased in infarcted LVs of AMI-induced rats, as compared to control sham-operated rats (*Fig. 5A-5D*). The levels of all these inflammatory markers were significantly decreased to their normal levels in the infarcted myocardium of the AMI + QUR-treated rats (*Fig. 5A-5D*). However, significantly higher levels of TNF-α, IL-6, nuclear activity of NF-κB, and nuclear protein level of NF-κB have been seen in the infarcted LVs of the AMI + S3I-201-treated rats as compared to all other groups. Interestingly, there was no significant variation in the levels of all these markers when the statistical analysis was conducted between AMI + S3I-201 and AMI + S31-201-treated rats (*Fig. 5A-5D*).

Quercetin improves the ultrastructural changes in the infarcted myocardium

Normal ultrastructures including normally appeared muscle fibers and bands (Z and H bands), dense mitochondria, and nuclei were seen in both the control and control + QUR sham-operated rats (*Fig. 6A* and *6B*). However, atrophied nuclei, chromatin condensation, damaged myofibrils and Z and H bands, swollen or shrunken and damage mitochondria, and increased collagen deposition with the appearance of myelin figures and apoptotic blebs were observed in the infarcted myocardium of AMI-induced rats (*Fig. 6C* and *6D*). Almost normal ultrastructures with condensed mitochondria and well-preserved H and Z bands were seen in the infarcted LVs obtained

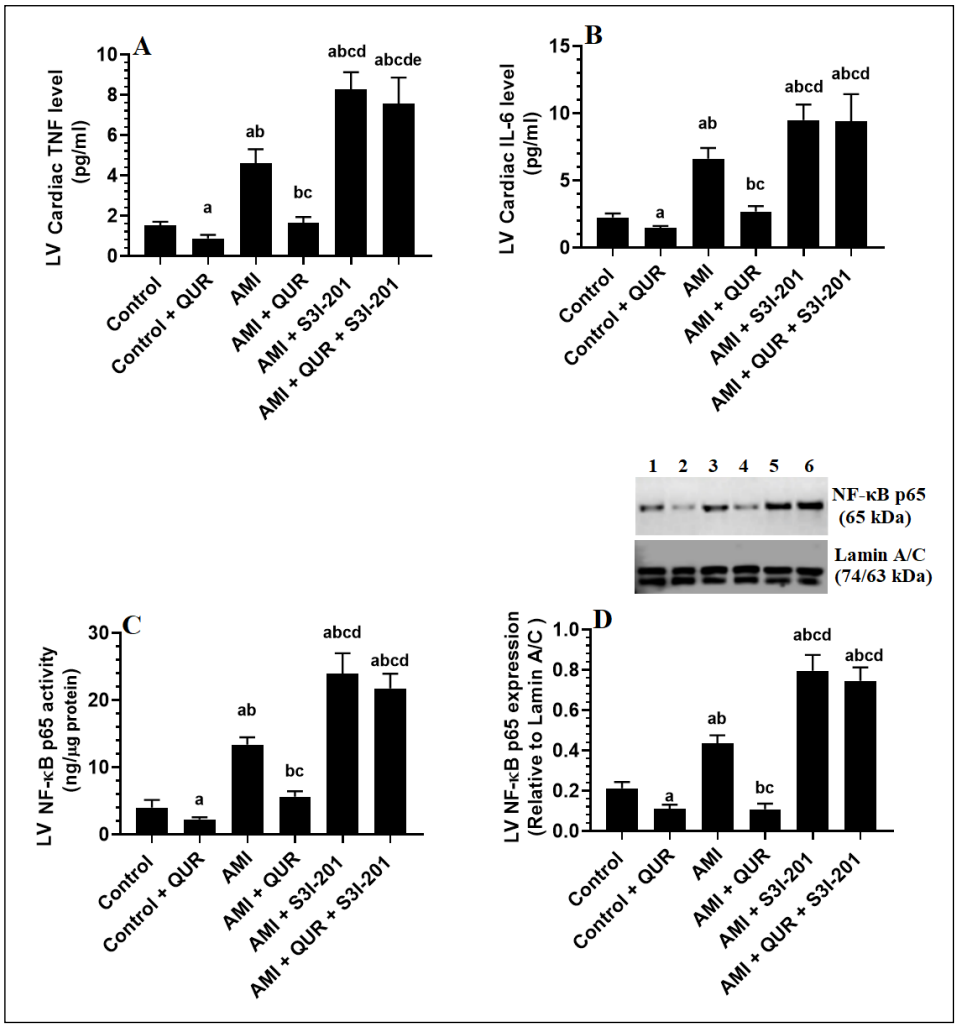

Fig. 5. Levels of tumor necrosis factor-alpha (TNF-α), interleukin-6 (IL-6), and nuclear activity and protein levels of nuclear factor-kappa B (NF-κB) in the left ventricles of all groups of rats. All data were analyzed by one-way ANOVA followed by Tukey's *t*-test. And the degree of significance was considered at $P < 0.05$. Data are presented as mean ± SD of n = 6/group. [a]: significantly different as compared to the control group (lane 1); [b]: significantly different as compared to control + quercetin (QUR) (lane 2); [c]: significantly different as compared to acute myocardial infarction (AMI)-induced rats (lane 3); [d]: significantly different as compared to AMI + QUR (lane 4). Lanes 5 and 6 represent MI + S31-201 and MI + QUR + S31-201, respectively.

from AMI + QUR-treated rats (*Fig. 7A*). A similar picture to the one seen in the infarcted LVs of the AMI-induced rats was observed in the LVs of AMI + S3I-treated rats but with an increased appearance of ghost bodies and collagen accumulation (*Fig. 7B* and *7C*). On the other hand, improvement in the H and Z bands with dense mitochondria and intact nuclei were observed in the AMI + QUR + SI3-201-treated rats (*Fig. 7D*). However, the structure and organization of the mitochondria remained abnormally appeared (*Fig. 7D*).

Quercetin prevents the opening of mtPTP in the infarcted myocardium

Levels of V_{max} (the decrease in the absorbance) and the time to reach V_{max} remained unchanged in the control + QUR sham-operated rats as compared to sham-operated control rats (*Fig. 8A* and *8B*). A significant increase in the levels of V_{max} with a parallel decrease in the levels of the time that is required to reach V_{max} was observed in the infarcted LVs of AMI-induced rats as compared to sham-operated control rats, thus indicating an increase in the opening of mtPTP (*Fig. 8A* and *8B*). The levels of both markers were completely returned to their levels in the LVs which were obtained from the AMI + QUR-treated rats (*Fig. 8A* and *8B*). On the other hand, V_{max} was significantly increased more and the time to reach V_{max} has significantly decreased more in AMI + S3I-201-treated rats as compared to AMI-treated rats (*Fig. 8A* and *8B*). A significant reduction in V_{max} and a significant increase in the time needed to reach V_{max} were observed in AMI + QUR + S3I-201 as compared to control rats. However, the levels of V_{max} remained significantly higher and the time to reach V_{max} remained significantly lower in AMI + QUR + S3I-201 as compared to AMI + QUR-treated rats (*Fig. 8A* and *8B*).

Quercetin suppresses markers of cell apoptosis in the left ventricles of rats partially in a STAT3-dependent manner

Protein levels of cleaved caspase-3 and cytochrome-c were not significantly changed but protein levels of Bax have significantly decreased in the LVs of control + QUR sham-operated rats as compared to sham-operated rats (*Fig. 9A* and *9B*). The protein levels of Bax, cleaved caspase-3, and cytochrome-C were significantly upregulated in the infarcted LVs of AMI-induced rats as compared to control sham-operated rats and were significantly decreased in the LVs of AMI + QUR-treated rats as compared to AMI-induced rats (*Fig. 9A* and *9B*). Although the levels of Bax and cytochrome-C were returned to their normal levels, the levels of cleaved caspase-3 in the LVs of AMI + QUR-treated rats remained slightly but significantly higher than its levels observed in the control sham-operated rats (*Fig. 9A* and *9B*). On the contrary, higher protein levels of Bax, cleaved caspase-3, and cytochrome-C were seen in the infarcted LVs of AMI + S3I-201 as compared to AMI-induced rats and all other groups (*Fig. 9A* and *9B*). A significant reduction in the levels of all these apoptotic markers was seen in the infarcted LVs obtained from AMI + QUR + S3I-201 as compared to AMI + S3I0201 (*Fig. 9A* and *9B*).

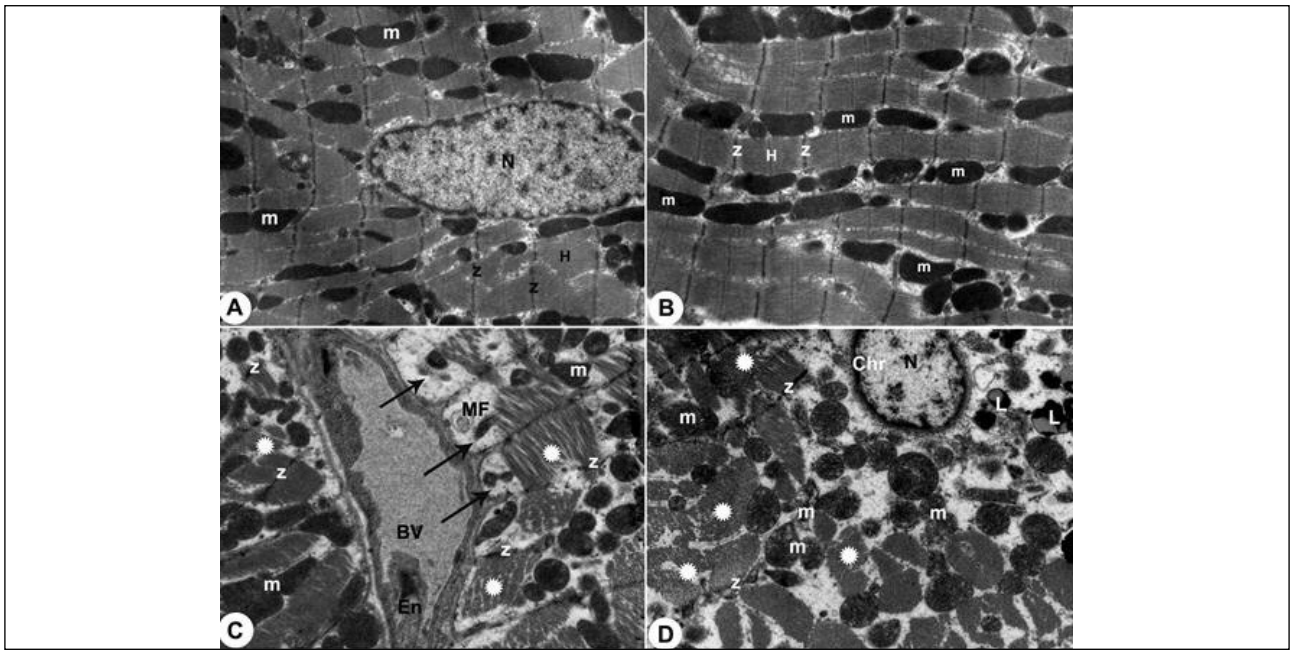

Fig. 6. Transmission electron micrographs (TEM) from the left ventricles of control sham-operated, control + quercetin (QUR) sham-operated, and acute myocardial infarction (AMI)-induced rats. (*A*) and (*B*): were taken from control sham-operated rats and control + quercetin (QUR)-treated rats and showed normal myocardial tissue with normal striated heart muscle fibers, dense mitochondria (m), and a clear nuclear (N) and muscle bands (Z and H bands). (*C*) and (*D*) were taken from AMI-induced rats and showed apoptotic myocardial cells (blebs) (arrow), degenerated cytoplasm with damaged myofibrils and collagen fiber accumulation (white asterisks), (arrows), myelin figures (MF), and atrophied nuclei (N) with the condensation of chromatin masses (Chr) on the nuclear membranes of these apoptotic cells. Fragmentation of muscle bands (Z and H bands) and swelled and shrunken and fragmented mitochondria (m) were also observed. × 10000.

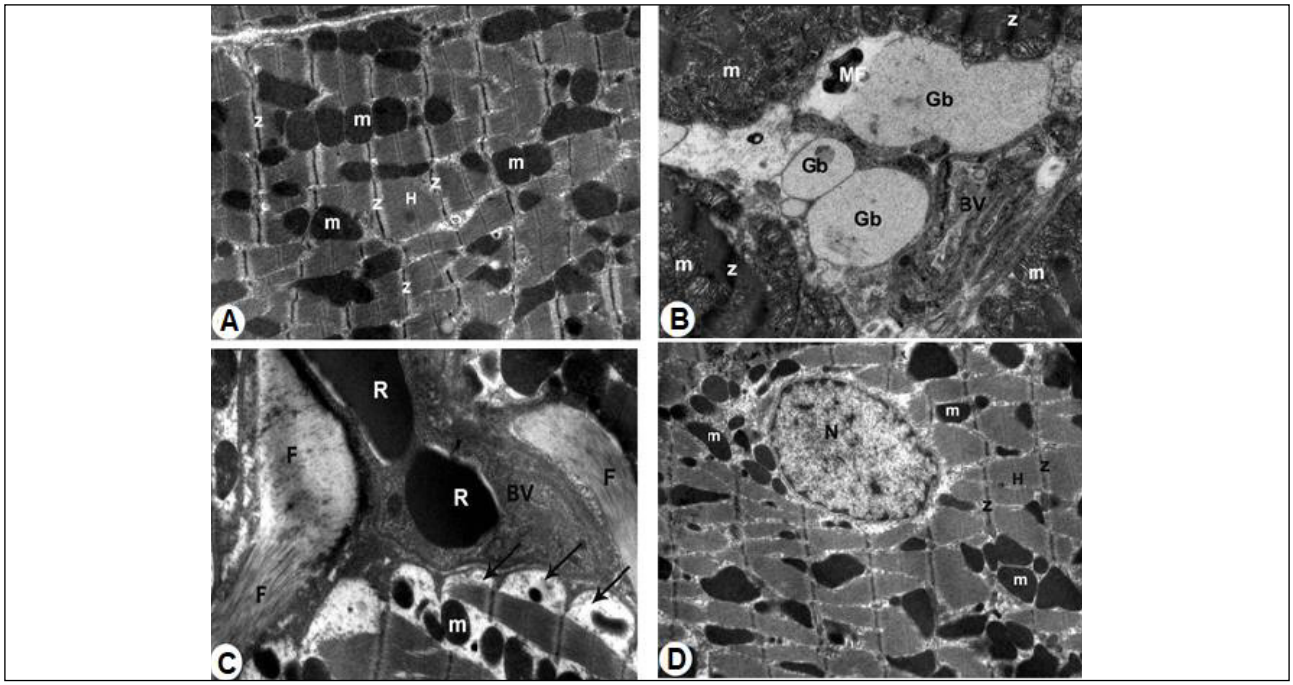

Fig. 7. Transmission electron micrographs (TEM) from the left ventricles of acute myocardial infarction (AMI) + quercetin (QUR), AMI + S3I-201 (a STAT3 inhibitor), and AMI + QUR + S3I-201-treated rats. (*A*): was taken from an AMI + QUR-treated rat and showed much improvement in the myocardial tissue structure with almost normally normal striated heart muscle fibers, dense mitochondria (m), and muscle bands (Z and H bands). (*B*) and (*C*): were taken from AMI + S31-201-treated rats and showed plenty of apoptotic myocardial blebs (arrow) and ghost bodies (Gb), shrunken blood vessel (BV), degenerated cytoplasm with the fragmentation of muscle bands (Z and H bands), and swollen mitochondria (m) with increased collagen fibers deposition (F). Also, myelin figures (MF) were observed squeezed in the interstitium between myocardial cells. (*D*) was taken from an AMI + QUR + S31-201-treated rat and showed an improvement in the structure of myofibrils and nucleus with dense mitochondria with intact Z and H bands. However, the distribution and shapes of the mitochondria were still abnormal. × 10000.

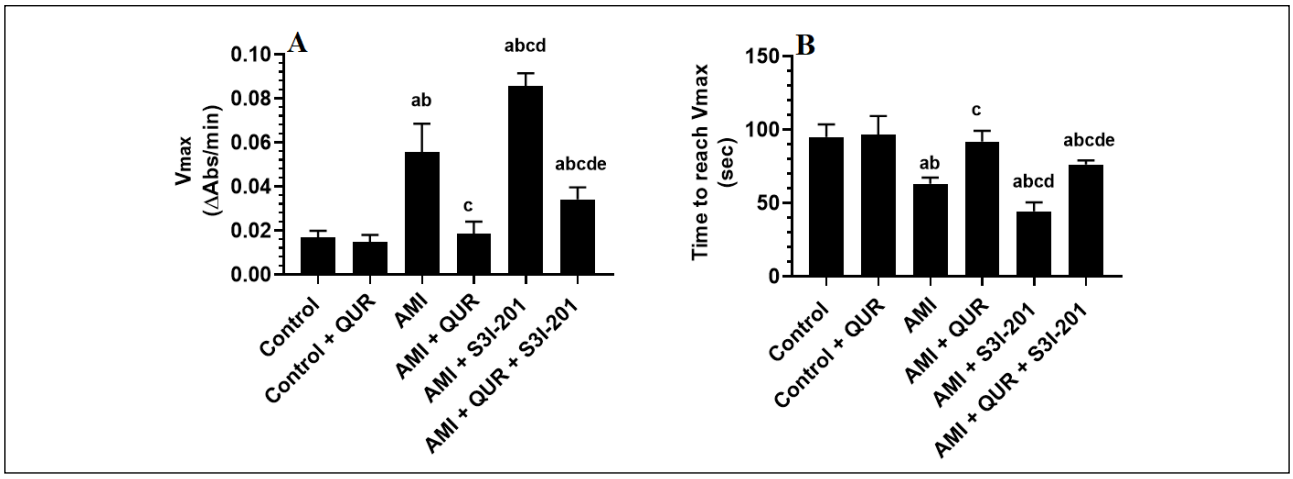

Fig. 8. The maximum decrease in the absorbance (V_{max}) and the time to reach V_{max} on the isolated mitochondria from the LVs of all groups of rats. All data were analyzed by one-way ANOVA followed by Tukey's *t*-test. And the degree of significance was considered at $P < 0.05$. Data are presented as mean ± SD of n = 6/group. [a]: significantly different as compared to the control group (lane 1); [b]: significantly different as compared to control + quercetin (QUR) (lane 2); [c]: significantly different as compared to acute myocardial infarction (AMI)-induced rats (lane 3); [d]: significantly different as compared to AMI + QUR (lane 4); [e]: significantly different as compared to MI + S31-201 (a stat inhibitor) (lanes 5). Lane 6 represents MI + QUR + S31-201.

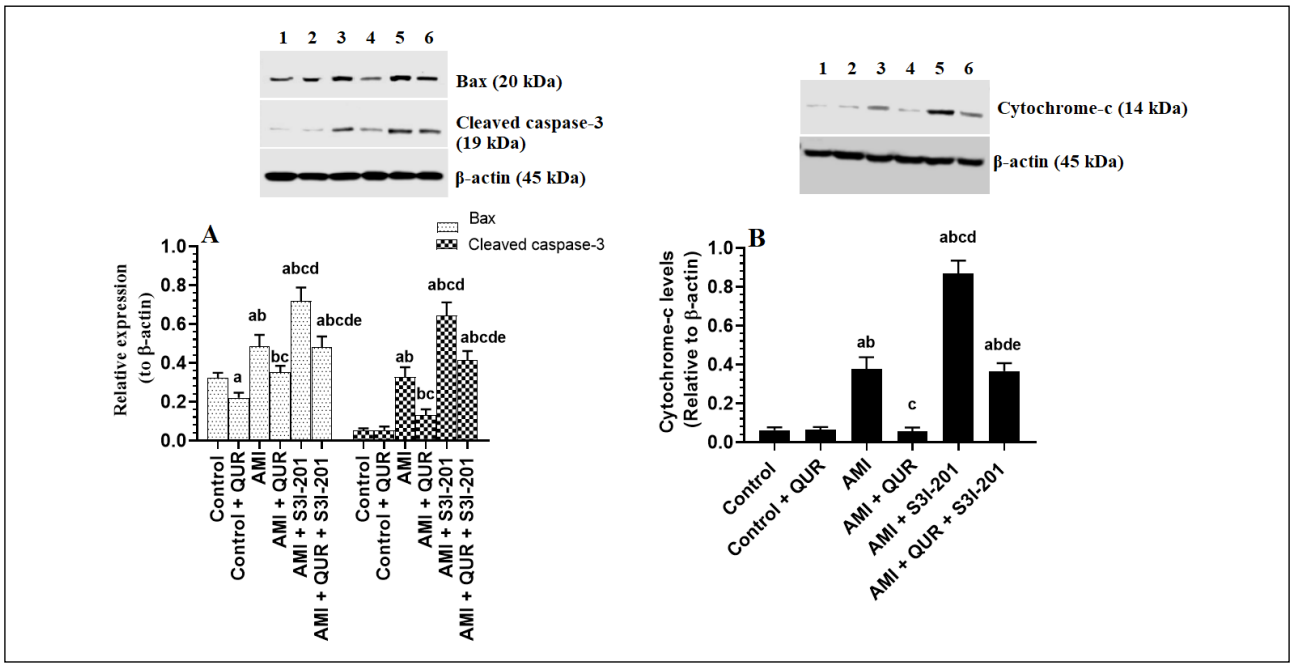

Fig. 9. Protein levels of Bax, cleaved caspase-3, and cytochrome-C in the LVs of all groups of rats. All data were analyzed by one-way ANOVA followed by Tukey's *t*-test. And the degree of significance was considered at $P < 0.05$. Data are presented as mean ± SD of n = 6/group. [a]: significantly different as compared to the control group (lane 1). [b]: significantly different as compared to control + quercetin (QUR) (lane 2); [c]: significantly different as compared to acute myocardial infarction (AMI)-induced rats (lane 3); [d]: significantly different as compared to AMI + QUR (lane 4); [e]: significantly different as compared to MI + S31-201 (a stat inhibitor) (lanes 5). Lane 6 represents MI + QUR + S31-201.

Quercetin stimulates STAT3 and suppress STAT1 in the left ventricles of rats independent of modulating JAK2

Total protein levels of JAK2, STAT1, and STAT3 were not significantly different in all groups of rats (*Fig. 10A-10C*). However, with no alteration in the expression of p-JAK2 ($Tyr^{1007/1008}$), the levels of p-STAT1 (Ser^{727}) were significantly decreased, and levels of p-STAT3 (Ser^{727}) were significantly increased in the LVs of control + QUR sham-operated rats as compared to the control sham-operated rats administered the vehicle (*Fig. 10A-10C*). Also, levels of p-JAK2 ($Tyr^{1007/1008}$), p-STAT1 (Ser^{727}), and STAT3 (Ser^{727}) were significantly increased in the infarcted myocardium of AMI-induced rats as compared to control sham-operated rats (*Fig. 10A-10C*). However, levels of p-STAT1 (Ser^{727}) were significantly decreased and levels of STAT3 (Ser^{727}) were significantly increased with stable levels of p-JAk2 ($Tyr^{1007/1008}$) in the LVs of AMI + QUR as compared to AMI-induced rats. The maximum increase in p-STAT3 (Ser^{727}) levels was observed in this group of rats (*Fig. 10A-10C*). On the contrary, levels of p-JAK2 ($Tyr^{1007/1008}$) were not significantly

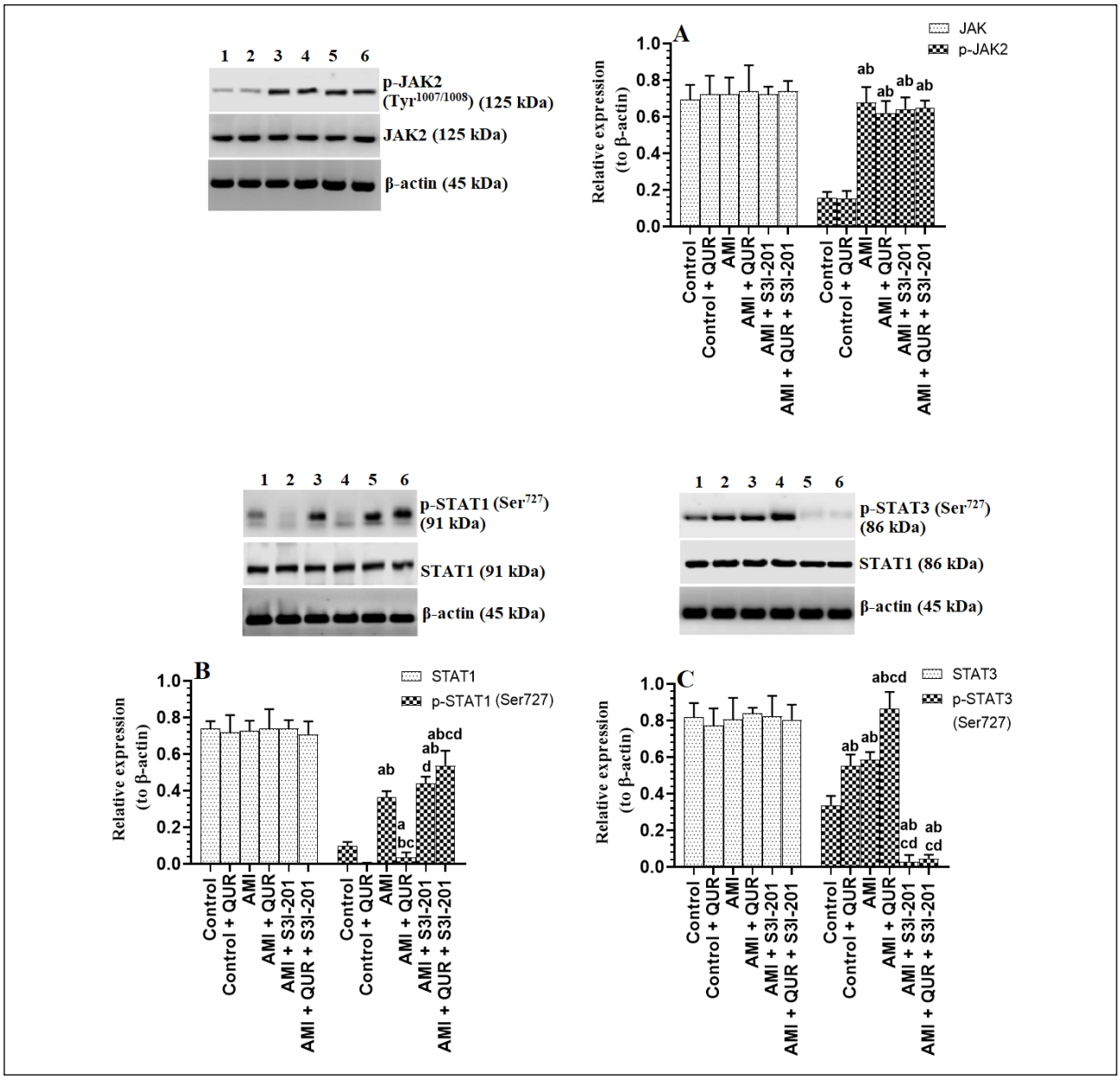

Fig. 10. Protein levels of total JAK2/p-JAK2 (Tyr$^{1007/1008}$), total STAT1/p-STAT1 (Ser^{727}), and total STAT3/p-STAT3 (Ser727) the LVs of all groups of rats. All data were analyzed by one-way ANOVA followed by Tukey's *t*-test. And the degree of significance was considered at $P < 0.05$. Data are presented as mean ± SD of n = 6/group. [a]: significantly different as compared to the control group (lane 1); [b]: significantly different as compared to control + quercetin (QUR) (lane 2); [c]: significantly different as compared to acute myocardial infarction (AMI)-induced rats (lane 3); [d]: significantly different as compared to AMI + QUR (lane 4); [e]: significantly different as compared to MI + S31-201 (a stat inhibitor) (lanes 5). Lane 6 represents MI + QUR + S31-201.

different but protein levels of p-STAT1 (Ser^{727}) were significantly higher with almost diminished levels of STAT3 (Ser^{727}) were observed in the LVs of the AMI + S3I-201 and AMI + QUR + S31-201-treated rats as compared to AMI-induced rats (*Fig. 10A-10C*).

DISCUSSION

In this study, we have confirmed that the activation of JAK2/STAT3 is a cardioprotective mechanism during the process of AMI. Besides, QUR cardioprotective effect is mediated by 1) suppressing the generation of ROS, 2) inhibiting mitochondria mtPTP opening, 3) increasing GSH and SOD levels, 4) inhibiting NF-κB, TNF-α, and IL-6, and 5) JAK2-independent activation of STAT3 and suppressing of STAT1. However, blunting the activity of STAT3 by S3I-201 partially prevented most of the effects afforded by QUR but completely prevented QUR-induced inhibition of NF-κB, the reduction in inflammatory cytokines levels, and activation of STAT1. Therefore, it seems reasonable that the anti-inflammatory effect of QUR is mediated by activating STAT3. Overall, the cardioprotective effect of QUR against AMI is mainly attributed to its potent antioxidant potential and activation of STAT3, A brief summary for the mechanism of action is shown in graphical abstract (*Fig. 11*).

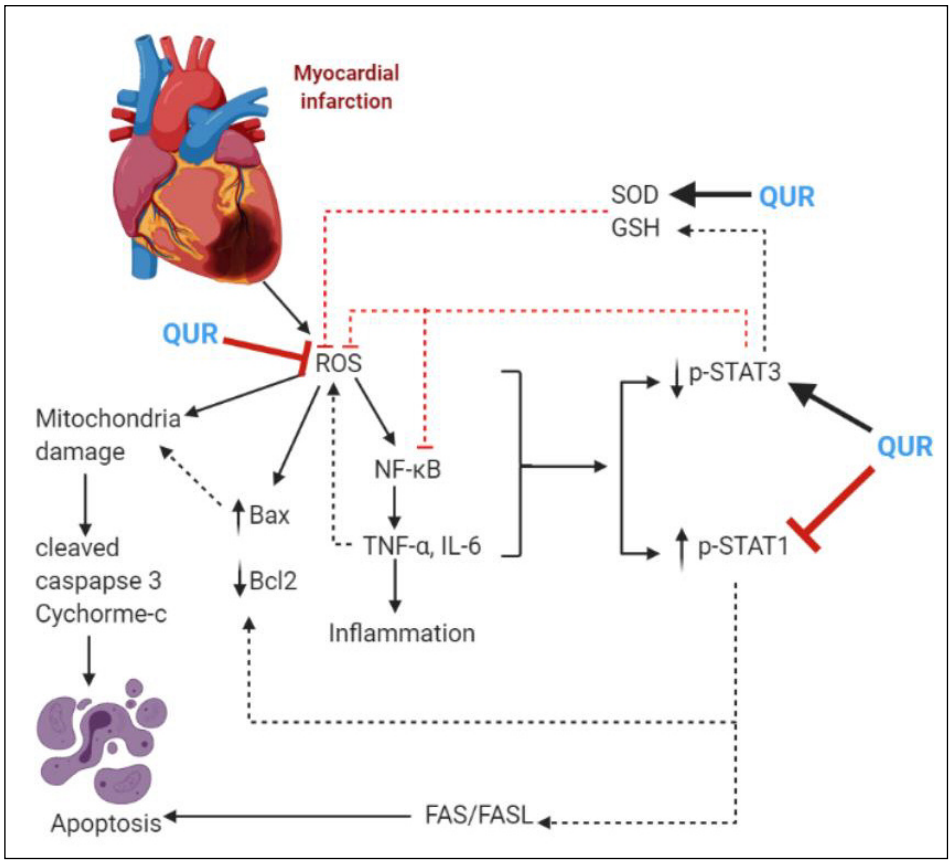

Fig. 11. A graphical abstract for the possible mechanisms behind the cardioprotective effect of quercetin against myocardial infarction. In brief, induction of cardiac ischemia produces large quantities of the reactive oxygen species (ROS) which activates the transcription factor, the nuclear factor kappa beta (NF-κB). This in turn provokes inflammatory cytokines production and cardiac inflammation. Besides, ROS can directly induce intrinsic cell death by inducing mitochondria, upregulation of Bax, and downregulation of Bcl2. ROS and inflammatory cytokines can also activate the pro-apoptotic STAT1 and inhibits the anti-apoptotic STAT3. QUR can protect against myocardial infarction by multiple interconnected mechanisms including suppressing the production of ROS, increasing the antioxidant levels, activating STAT4, and inhibiting STAT1.

The LAD ligation protocol in rodents remains the most acceptable method to induce and study the pathophysiology of AMI as it produces similar clinical manifestations and activates similar cardiac pathways like those seen in humans (42). Oxidative stress due to overproduction of ROS stress and inflammation due to activation of NF-κB are two major related mechanisms that are activated early during AMI and are responsible for all other adverse effects including cardiomyocyte death, infarct expansion, and remodeling (43-47). ROS are generated during cardiac ischemia due to multiple-interconnected mechanisms including infiltrating macrophages, mitochondria damaged, impaired oxidative phosphorylation, the activation of ROS-generating enzymes (i.e. xanthine oxidoreductase, NADPH oxidase, NO synthases (NOS), cyclooxygenase (COX)), catecholamines auto-oxidation, and Ca^{+2} overload (48, 49). However, ROS originated in the mitochondria is believed to be the initial and key player events that trigger all these other events in the infarcted myocardium (48, 49). Besides, the ROS triggers sustained myocardial inflammatory response by promoting inflammasome assembly and activating NF-κB in a variety of cardiac cells including surviving cardiomyocytes, macrophages, fibroblasts, and infiltrated neutrophils, which together increase the levels of the inflammatory cytokine and induces leukocyte chemotaxis, complement activation, expression of adhesive molecules, and ROS generation will in the infarcted area (47-49).

In the same line with all these studies, AMI-induced by LAD ligation in this study not only induced a large infarction and impaired LV function in rats but also induced severe damage of the cardiac myofibrils, induced severe mitochondria damage, increased ROS generation, enhanced lipid peroxidation, overwhelmed GSH and SOD levels, and increased the activation of NF-κB and the levels of TNF-α and IL-6. These data confirm the crucial close roles of oxidative stress and inflammation in cardiac damage and the pathogenesis of MI post-induction of AMI. On the other hand, pre-treating the ischemic rats with QUR almost preserved all these events and returned their levels to those seen in the control rats. Also, QUR increased the levels of SOD and GSH and decreased the activation of NF-κB and levels of TNF-α and IL-6 in the hearts of control rats. Based on these data, it seems reasonable that the protective effect of QUR against acute MI in rats includes antioxidant and anti-inflammatory effects mediated by upregulation of endogenous antioxidants and downregulation/inhibition of NF-κB. Although some studies have indicated that activation of NF-κB could be a protective mechanism during AMI due to prompting the survival pathway (50). Our data suggest the opposite and support that the activation of NF-κB is determinable. In support, improved early survival and LV function, reduced infarction size, and less inflammatory cytokines and cardiomyocytes apoptosis were seen after inhibiting NF-κB or in the hearts of NF-κB p50 null mice after exposure to cardiac I/R injury or MI (51-54).

These data are not strange given the well-known antioxidant and inflammatory cardioprotective effect of QUR in the heart and other tissues MI and I/R injury (55, 56). Indeed, QUR antioxidant effect is mediated by scavenging hydroxyl and superoxide anion radicals, chelating transition metal ions (i.e. iron), and inhibiting ROS-generating enzymes including xanthine oxidase and iNOS (57, 58). Besides, QUR preserved cardiac structure and function in isoprenaline-induced myocardial infarction in rats by suppressing Ca^{+2} overload (56) and inhibiting the generation of ROS and TNF-α (32). Similar effects of QUR were also demonstrated in an animal model of atherosclerosis (55). Also, QUR can downregulate iNOS and suppress the activation of NF-κB and the generation of several inflammatory cytokines from the macrophages, *in vivo,* and *in*

vitro (59, 60). Besides, QUR preserved cardiac function and hemodynamic parameters by increasing the levels of the anti-inflammatory cytokine, IL-10 in rats exposed to I/R (24). Furthermore, QUR and its derivative dihydroquercetin, prevented cardiac damage mainly by increasing the expression of endogenous antioxidant enzymes by upregulation of heme oxygenase-1 (HO-1) and the nuclear factor- erythroid 2-related factor (Nrf2) in the hearts of animals exposed to chronic stress and I/R or treated with doxorubicin (33, 61).

However, necrosis and both forms of apoptosis (intrinsic and extrinsic) are directly activated in the infarcted myocardium after induction of cardiac ischemia and were proposed to be the major cause of cardiomyocyte loss and LV dysfunction (44, 62). The mitochondria damage, mainly due to ROS, was shown to mediate both necrosis and apoptosis during this process (44). Generally speaking, intrinsic cell apoptosis occurs mainly due to permeabilization of the outer mitochondrial membrane as a result of an imbalance in the expression of pro-apoptotic and anti-apoptotic proteins (Bax and Bcl-2, respectively) which leads to the release of mitochondria apoptotic factors (i.e. cytochrome-C and inhibitor of apoptosis (IAP) binding protein) and subsequently caspases activation (63). In this regard, it was shown that ischemia-induced ROS rapidly activated p53 and subsequently upregulates Bax to induce mitochondria permeabilization (62). Also, ROS can induce cardiomyocyte necrosis by increasing intracellular Ca^{2+} overload due to decreasing Ca^{2+} efflux (sequestration) mediated by suppressing the sarcolemma Ca^{2+}-pump ATPase (SERCA) and increasing Ca^{2+} influx through inhibiting the Na^{+}/K ATPase activity. Accordingly, Ca^{+2} entry to the mitochondria is increased leading to the opening of the mitochondrial permeability transition pore (MPTP), ATP depletion, water influx (swelling), loss of plasma membrane integrity (rupture), and release of pro-apoptotic factors (i.e. cytochrome C) and caspases activation (62, 64, 65). Besides, it has been reported that intrinsic and extrinsic cell death pathways may amplify the opening of the mtPTP through the pro-apoptotic Bcl-2 family protein, Bid (66).

In this study, both necrosis and intrinsic cell apoptosis were evidenced in the infarcted areas of the MI groups given the significant increase in serum levels of LDH, troponin-I, and CKMB, as well as the significant increase in protein levels of Bax, cytochrome-C, and cleaved caspase-3. Besides, cardiomyocytes from the infarcted area of the rats' hearts showed a significant increase in mtPTP opening as evidenced by the rapid decrease in absorbance (V_{max}) and the faster time to reach (V_{max}). However, all these events were completely reversed by QUR pre-treatment. Although such anti-apoptotic effect of QUR could be explained as a secondary effect due to its antioxidant and ROS scavenging effects, the significant reduction in Bax levels in the QUR-treated control hearts suggests a regulatory effect of QUR on Bax expression which also participate in its anti-apoptotic effect which explained later by modulating STAT3 and STAT1 activities.

Nonetheless, the precise molecular signaling pathways behind the anti-oxidant, anti-inflammatory, and anti-apoptotic effects of QUR still largely unknown. Therefore, in this study, we have targeted the JAK2/STAT1/STAT3 pathway given its important role in the pathogenesis of AMI and its wide-range roles in oxidative stress, inflammation, and apoptosis (4, 10, 16). In the ischemic cardiomyocytes, the activation of this pathway is mainly triggered by the higher levels of ROS, IL-6, and ANGII (4, 10, 67). All JAK members, as well as STAT1/STAT3, are activated in the infarcted myocardium during cardiac ischemia and remain significantly high up to 1 week (68-70). Under stress, the cytoplasm-resident STAT3 is rapidly phosphorylated at specific serine and tyrosine residues and translocated to the nucleus and the mitochondria to regulate gene expression and preserving mitochondria integrity (10). Within this view, the phosphorylation of STAT3 at Tyr^{705} is important for its nuclear and mitochondria translocation, as well as binding with the DNA (10). However, the Ser^{727} phosphorylation is needed for the maximum transcriptional activity rather than binding DNA (4, 10). On the other hand, STAT1 is activated by phosphorylation at both Ser^{727} and Tyr^{701}, where the phosphorylation of SER^{727} is required for full transcriptional activity (16).

In the cardiomyocytes, like most cells, STAT3 and STAT1 exert contradictory effects. Accordingly, STAT1 activates cell apoptosis by inducing the transcription of a variety of pro-apoptotic factors including caspase-1, Fas, FasL, p53, and Bax, and inducing apoptotic autophagy (13, 16, 69, 70). On the other hand, STAT3 has cytoprotective effects that are associated with a reduction of the myocardial infarction with potent antioxidant, anti-inflammatory, and anti-apoptotic effects (4, 10). Although the initial rapid activation of STAT3 is required for the early synthesis of inflammatory cytokines to facilities myocardium recovery, it suppresses inflammation by suppressing NF-κB activity (71, 72). Also, STAT3 has potent anti-apoptotic potential by increasing the expression of anti-apoptotic genes including Bcl-2, Bcl-XL, and MCl-1 (73) phosphorylation-induced suppression of Bad (74), and (c-FLIP), and preventing ROS/Ca^{+2}-induced mitochondrial mtPTP opening (75, 76). STAT3 also modulated the cardiac microenvironment by preserving erythropoietin levels and endothelial differentiation of cardiac progenitor cells (77). Besides, STAT3 induces cytoprotective autophagy by upregulating multiple autophagy-related genes (78-80). Also, STAT3 cardioprotective effect is mediated by preserving cardiac metabolism (5). Furthermore, STAT-3 antioxidant potential is mediated by reducing ROS generation from the mitochondria and upregulation of the expression of Nrf-2, HO-1, and numerous antioxidants genes (i.e. metallothioneins and SOD) (81-83).

In this study, the activities of JAK2, STAT1 (Ser727), and STAT3 (Ser272) were also significantly increased in the infarcted myocardium, 24 h after the induction of AMI which supports the above-mentioned studies. Such an increase in the activities of STAT1 and STAT3 could be explained by ischemia-induced ROS, TNF-α, and IL-6. However, the contribution of other factors such as ANG II and other molecules should not be neglected. However, our data suggest that the activation of STAT3 in the hearts of AMI-induced rats is a protective signal as suppressing STAT3 in the ischemic hearts by S3I-201 exaggerated the infarct area and serum levels of cardiac markers, increased the reduction in levels of GSH and SOD, and increased ROS, the activation of NF-κB, levels of inflammatory cytokines, the opening of the mtPTP, and protein levels of Bax, cleaved caspase-3 and cytochrome-C, as compared to MI-induced rats. Therefore, it seems reasonable that the observed increase in apoptotic factors is mediated by the increase in STAT-1 levels whereas STAT3 is counteracting this by exerting anti-oxidant, anti-inflammatory, and anti-apoptotic effects.

On the other hand, QUR protective effect was associated with increasing the activity of STAT3 and suppressing that of STAT1. Indeed, QUR increased the activation of STAT3 and reduced the activation of STAT1 not only in the infarcted myocardium but also in the hearts of the control rats. These effects were independent of modulating the activity of JAK2 as stable levels of this protein were reported in control and AMI-induced rats, which pre-treated with QUR. However, it has been shown that a negative cross-talk exists between STAT-1 and STAT3 where both proteins can negatively affect each other (16). Indeed, higher activation of STAT3 was reported in cells lacking STAT-1 and in the infarcted myocardium (16, 84). Based on the data in our hand, it is very difficult for us to determine if the QUR effect is mediated by suppression of STAT1 and/or activating STAT3. Interestingly, GSH levels were shown to be positively associated

with STAT3 levels and activation. In this regard, glutathione monoethyl ester and N-acetyl-cysteine (NAC) (both are GSH precursors) increased the activation and prevented the inhibition of STAT3 whereas thiolate-targeting electrophiles inhibited STAT3 activation (85, 86). Interestingly, levels of STAT1 are not affected by intracellular levels of GSH (85). Given that QUR didn't affect inflammatory levels of TNF-α and IL-6 neither the levels of ROS in the control hearts, it could be possible that QUR activated STAT3 and subsequently inhibited STAT3 by increasing GSH levels, possibly due to regulation of GSH synthesis. Further studies on this are needed to reveal this.

In conclusion, the finding in our hand still very interesting and suggest that consumption of QUR protects against MI by suppressing oxidative stress and inflammation mediated by increasing levels of antioxidants and activation of STAT3. Further clinical trials are highly encouraged to validate these findings and trying to develop effective cardioprotective drugs.

Source of funding: This research was funded by the Deanship of Scientific Research at Princess Nourah bint Abdulrahman University, through the Research Funding Program (Grant No # FRP-1442-18).

Acknowledgement: The authors would like to thank the Deanship of Scientific Research at Princess Nourah bint Abdulrahman University, Riyadh, Saudi Arabia, through the Research Funding Program (Grant No # FRP-1442-18) for funding this study.

Conflict of interests: None declared.

REFERENCES

1. Thygesen K, Alpert JS, Jaffe AS, *et al*. Fourth universal definition of myocardial infarction. *Circulation*. 2018; 138: e618-e651. doi: 10.1161/CIR.0000000000000617
2. McMurray J, McLay J, Chopra M, Bridges A, Belch JJ. Evidence for enhanced free radical activity in chronic congestive heart failure secondary to coronary artery disease. *Am J Cardiol* 1990; 65: 1261-1262.
3. Jia Y, Castellanos J, Wang C, *et al*. Mitogen-activated protein kinase signaling in male germ cell apoptosis in the rat. *Biol Reprod* 2009; 80: 771-780.
4. O'Sullivan KE, Breen EP, Gallagher HC, Buggy DJ, Hurley JP. Understanding STAT3 signaling in cardiac ischemia. *Basic Res Cardiol* 2016; 111: 27. doi: 10.1007/s00395-016-0543-8
5. Harhous Z, Booz GW, Ovize M, Bidaux G, Kurdi M. An update on the multifaceted roles of STAT3 in the heart. *Front Cardiovasc Med* 2019; 6: 150. doi: 10.3389/fcvm.2019.00150
6. Kiu H, Nicholson SE. Biology and significance of the JAK/STAT signalling pathways. *Growth Factors* 2012; 30: 88-106.
7. Pan J, Fukuda K, Kodama H, *et al*. Role of angiotensin II in activation of the JAK/STAT pathway induced by acute pressure overload in the rat heart. *Circ Res* 1997; 81: 611-617.
8. Booz GW, Day JN, Baker KM. Interplay between the cardiac renin angiotensin system and JAK-STAT signaling: role in cardiac hypertrophy, ischemia/reperfusion dysfunction, and heart failure. *J Mol Cell Cardiol* 2002; 34: 1443-1453.
9. Kurdi M, Booz GW. Can the protective actions of JAK-STAT in the heart be exploited therapeutically? Parsing the regulation of interleukin-6-type cytokine signaling. *J Cardiovasc Pharmacol* 2007; 50: 126-141.
10. Zouein FA, Altara R, Chen Q, Lesnefsky EJ, Kurdi M, Booz GW. Pivotal importance of STAT3 in protecting the heart from acute and chronic stress: new advancement and unresolved issues. *Front Cardiovasc Med* 2015; 2: 36. doi: 10.3389/fcvm.2015.00036
11. Fuchs M, Hilfiker A, Kaminski K, *et al*. Role of interleukin-6 for LV remodeling and survival after experimental myocardial infarction. *FASEB J* 2003; 17: 2118-2120.
12. McCormick J, Barry SP, Sivarajah A, *et al*. Free radical scavenging inhibits STAT phosphorylation following in vivo ischemia/reperfusion injury. *FASEB J* 2006; 20: 2115-2117.
13. Stephanou A, Scarabelli TM, Brar BK, *et al*. Induction of apoptosis and Fas receptor/Fas ligand expression by ischemia/reperfusion in cardiac myocytes requires serine 727 of the STAT-1 transcription factor but not tyrosine 701. *J Biol Chem* 2001; 276: 28340-28347.
14. Townsend PA, Scarabelli TM, Davidson SM, Knight RA, Latchman DS, Stephanou A. STAT-1 interacts with p53 to enhance DNA damage-induced apoptosis. *J Biol Chem* 2004; 279: 5811-5820.
15. McCormick J, Suleman N, Scarabelli TM, Knight RA, Latchman DS, Stephanou A. STAT1 deficiency in the heart protects against myocardial infarction by enhancing autophagy. *J Cell Mol Med* 2012; 16: 386-393.
16. Eid RA, Alkhateeb MA, Eleawa S, *et al*. Cardioprotective effect of ghrelin against myocardial infarction-induced left ventricular injury via inhibition of SOCS3 and activation of JAK2/STAT3 signaling. *Basic Res Cardiol* 2018; 113: 13. doi: 10.1007/s00395-018-0671-4
17. Boengler K, Buechert A, Heinen Y, *et al*. Cardioprotection by ischemic postconditioning is lost in aged and STAT3-deficient mice. *Circ Res* 2008; 102: 131-135.
18. Gao S, Zhan L, Yang Z, *et al*. Remote limb ischaemic postconditioning protects against myocardial ischaemia/reperfusion injury in mice: activation of JAK/STAT3-mediated Nrf2-antioxidant signalling. *Cell Physiol Biochem* 2017; 43: 1140-1151.
19. Zouein FA, Kurdi M, Booz GW. Dancing rhinos in stilettos: the amazing saga of the genomic and nongenomic actions of STAT3 in the heart. *JAKSTAT* 2013; 2: e24352. doi: 10.4161/jkst.24352
20. Zorniak M, Porc MP, Krzeminski TF. Hawthorn revisited: time- and dose-dependent cardioprotective action of WS-1442 special extract in the reperfusion-induced arrhythmia model in rats in vivo. *J Physiol Pharmacol* 2019; 70: 307-314.
21. Anand David AV, Arulmoli R, Parasuraman S. Overviews of biological importance of quercetin: a bioactive flavonoid. *Pharmacogn Rev* 2016; 10: 84-89.
22. Tang J, Lu L, Liu Y, *et al*. Quercetin improve ischemia/reperfusion-induced cardiomyocyte apoptosis in vitro and in vivo study via SIRT1/PGC-1α signaling. *J Cell Biochem* 2019; 120: 9747-9757.
23. Li M, Jiang Y, Jing W, Sun B, Miao C, Ren L. Quercetin provides greater cardioprotective effect than its glycoside derivative rutin on isoproterenol-induced cardiac fibrosis in the rat. *Can J Physiol Pharmacol* 2013; 91: 951-959.
24. Li B, Yang M, Liu JW, Yin GT. Protective mechanism of quercetin on acute myocardial infarction in rats. *Genet Mol Res* 2016; 15: 15017117. doi: 10.4238/gmr.15017117
25. Liu X, Yu Z, Huang X, *et al*. Peroxisome proliferator-activated receptor γ (PPARγ) mediates the protective effect of quercetin against myocardial ischemia-reperfusion injury via suppressing the NF-κB pathway. *Am J Transl Res* 2016; 8: 5169-5186.
26. Jin HB, Yang YB, Song YL, Zhang YC, Li YR. Protective roles of quercetin in acute myocardial ischemia and reperfusion injury in rats. *Mol Biol Rep* 2012; 39: 11005-11009.
27. Chen YW, Chou HC, Lin ST, *et al*. Cardioprotective effects of quercetin in cardiomyocyte under ischemia/reperfusion

injury. *Evid Based Complement Alternat Med* 2013; 2013: 364519. doi: 10.1155/2013/364519
28. Jurca T, Baldea I, Filip GA, *et al*. The effect of Tropaeolum majus L. on bacterial infections and in vitro efficacy on apoptosis and DNA lesions in hyperosmotic stress. *J Physiol Pharmacol* 2018; 69: 391-401.
29. Igbe I, Shen XF, Jiao W, *et al*. Dietary quercetin potentiates the antiproliferative effect of interferon-α in hepatocellular carcinoma cells through activation of JAK/STAT pathway signaling by inhibition of SHP2 phosphatase. *Oncotarget* 2017; 8: 113734-113748.
30. Jiang H, Yamashita Y, Nakamura A, Croft K, Ashida H. Quercetin and its metabolite isorhamnetin promote glucose uptake through different signalling pathways in myotubes. *Sci Rep* 2019; 9: 2690. doi: 10.1038/s41598-019-38711-7
31. Liu YR, Xu HM. Protective effect of necrostatin-1 on myocardial tissue in rats with acute myocardial infarction. *Genet Mol Res* 2016; 15: doi: 10.4238/gmr.15027298
32. Zaafan MA, Zaki HF, El-Brairy AI, Kenawy SA. Protective effects of atorvastatin and quercetin on isoprenaline-induced myocardial infarction in rats. *Bull Fac Pharm Cairo Univ* 2013; 51: 35-41.
33. Bin-Jaliah I. Quercetin inhibits chronic stress-induced myocardial infarction in rats. *Int J Morphol* 2017; 35: 1363-1369.
34. Mir SA, Chatterjee A, Mitra A, Pathak K, Mahata SK, Sarkar S. Inhibition of signal transducer and activator of transcription 3 (STAT3) attenuates interleukin-6 (IL-6)-induced collagen synthesis and resultant hypertrophy in rat heart. *J Biol Chem* 2012; 287: 2666-2677.
35. Song M, Wang C, Yang H, *et al*. P-STAT3 Inhibition Activates endoplasmic reticulum stress-induced splenocyte apoptosis in chronic stress. *Front Physiol* 2020; 11: 680. doi: 10.3389/fphys.2020.00680
36. Pan Z, Sun X, Ren J, *et al*. miR-1 exacerbates cardiac ischemia-reperfusion injury in mouse models. *PLoS One* 2012; 7: e50515. doi: 10.1371/journal.pone.0050515
37. Eid RA, Bin-Meferij MM, El-Kott AF, *et al*. Exendin-4 protects against myocardial ischemia-reperfusion injury by upregulation of SIRT1 and SIRT3 and activation of AMPK. *J Cardiovasc Transl Res* 2020; Apr. 1: doi: 10.1007/s12265-020-09984-5
38. Adhihetty PJ, Ljubicic V, Menzies KJ, Hood DA. Differential susceptibility of subsarcolemmal and intermyofibrillar mitochondria to apoptotic stimuli. *Am J Physiol Cell Physiol* 2005; 289: C994-C1001.
39. Kavazis AN, McClung JM, Hood DA, Powers SK. Exercise induces a cardiac mitochondrial phenotype that resists apoptotic stimuli. *Am J Physiol Heart Circ Physiol* 2008; 294: H928-H935.
40. Kavazis AN, Morton AB, Hall SE, Smuder AJ. Effects of doxorubicin on cardiac muscle subsarcolemmal and intermyofibrillar mitochondria. *Mitochondrion* 2017; 34: 9-19.
41. Mostafa DG, Khaleel EF, Badi RM, Abdel-Aleem GA, Abdeen HM. Rutin hydrate inhibits apoptosis in the brains of cadmium chloride-treated rats via preserving the mitochondrial integrity and inhibiting endoplasmic reticulum stress. *Neurol Res* 2019; 41: 594-608.
42. Kolk MV, Meyberg D, Deuse T, *et al*. LAD-ligation: a murine model of myocardial infarction. *J Vis Exp* 2009; 32: 1438. doi: 10.3791/1438
43. Berg K, Jynge P, Bjerve K, Skarra S, Basu S, Wiseth R. Oxidative stress and inflammatory response during and following coronary interventions for acute myocardial infarction. *Free Radic Res* 2005; 39: 629-636.
44. Frangogiannis NG. Pathophysiology of myocardial infarction. *Compr Physiol* 2015; 5: 1841-1875.
45. Moris D, Spartalis M, Spartalis E, *et al*. The role of reactive oxygen species in the pathophysiology of cardiovascular diseases and the clinical significance of myocardial redox. *Ann Transl Med* 2017; 5: 326. doi: 10.21037/atm.2017.06.27
46. Aimo A, Castiglione V, Borrelli C, *et al*. Oxidative stress and inflammation in the evolution of heart failure: From pathophysiology to therapeutic strategies. *Eur J Prev Cardiol* 2020; 27: 494-510.
47. Ahmed LA, Hassan OF, Galal O, Mansour DF, El-Khatib A. Beneficial effects of benfotiamine, a NADPH oxidase inhibitor, in isoproterenol-induced myocardial infarction in rats. *PLoS One* 2020; 15: e0232413. doi: 10.1371/journal.pone.0232413
48. Neri M, Fineschi V, Di Paolo M, *et al*. Cardiac oxidative stress and inflammatory cytokines response after myocardial infarction. *Curr Vasc Pharmacol* 2015; 13: 26-36.
49. Gonzalez-Montero J, Brito R, Gajardo AI, Rodrigo R. Myocardial reperfusion injury and oxidative stress: therapeutic opportunities. *World J Cardiol* 2018; 10: 74-86.
50. Misra A, Haudek SB, Knuefermann P, *et al*. Nuclear factor-kappaB protects the adult cardiac myocyte against ischemia-induced apoptosis in a murine model of acute myocardial infarction. *Circulation* 2003; 108: 3075-3078.
51. Frantz S, Hu K, Bayer B, *et al*. Absence of NF-kappaB subunit p50 improves heart failure after myocardial infarction. *FASEB J* 2006; 20: 1918-1920.
52. Moss NC, Stansfield WE, Willis MS, Tang RH, Selzman CH. IKKbeta inhibition attenuates myocardial injury and dysfunction following acute ischemia-reperfusion injury. *Am J Physiol Heart Circ Physiol* 2007; 293: H2248-H2253.
53. Zhang XQ, Tang R, Li L, *et al*. Cardiomyocyte-specific p65 NF-κB deletion protects the injured heart by preservation of calcium handling. *Am J Physiol Heart Circ Physiol* 2013; 305: H1089-H1097.
54. Maimaitiaili A, Li J, Aibibula A, Abudureheman M. Inhibition of nuclear factor kappa B pathway protects myocardial ischemia/reperfusion injury in rats under treatment with abnormal savda munziq. *Am J Transl Res* 2018; 10: 77-85.
55. Sevastre-Berghian AC, Toma VA, Sevastre B, *et al*. Characterization and biological effects of Hypericum extracts on experimentally-induced - anxiety, oxidative stress and inflammation in rats. *J Physiol Pharmacol* 2018; 69: 789-800.
56. Punithavathi VR, Stanely Mainzen Prince P. The cardioprotective effects of a combination of quercetin and α-tocopherol on isoproterenol-induced myocardial infarcted rats. *J Biochem Mol Toxicol* 2011; 25: 28-40.
57. Takizawa S, Fukuyama N, Hirabayashi H, *et al*. Quercetin, a natural flavonoid, attenuates vacuolar formation in the optic tract in rat chronic cerebral hypoperfusion model. *Brain Res* 2003; 980: 156-160.
58. Heo HJ, Lee CY. Protective effects of quercetin and vitamin C against oxidative stress-induced neurodegeneration. *J Agric Food Chem* 2004; 52: 7514-7517.
59. Wadsworth TL, Koop DR. Effects of the wine polyphenolics quercetin and resveratrol on pro-inflammatory cytokine expression in RAW 264.7 macrophages. *Biochem Pharmacol* 1999; 57: 941-949.
60. Comalada M, Camuesco D, Sierra S, *et al*. In vivo quercitrin anti-inflammatory effect involves release of quercetin, which inhibits inflammation through down-regulation of the NF-kappaB pathway. *Eur J Immunol* 2005; 35: 584-592.
61. Shu Z, Yang Y, Yang L, Jiang H, Yu X, Wang Y. Cardioprotective effects of dihydroquercetin against ischemia reperfusion injury by inhibiting oxidative stress and endoplasmic reticulum stress-induced apoptosis via the PI3K/Akt pathway. *Food Funct* 2019; 10: 203-215.

62. Webster KA. Mitochondrial membrane permeabilization and cell death during myocardial infarction: roles of calcium and reactive oxygen species. *Future Cardiol* 2012; 8: 863-884.
63. Eleawa SM, Alkhateeb M, Ghosh S, *et al*. Coenzyme Q10 protects against acute consequences of experimental myocardial infarction in rats. *Int J Physiol Pathophysiol Pharmacol* 2015; 7: 1-13.
64. Krijnen PA, Nijmeijer R, Meijer CJ, Visser CA, Hack CE, Niessen HW. Apoptosis in myocardial ischaemia and infarction. *J Clin Pathol* 2002; 55: 801-811.
65. Hool LC. The L-type Ca(2+) channel as a potential mediator of pathology during alterations in cellular redox state. *Heart Lung Circ* 2009; 18: 3-10.
66. Kaufmann T, Strasser A, Jost PJ. Fas death receptor signalling: roles of Bid and XIAP. *Cell Death Differ* 2012; 19: 42-50.
67. Wang M, Zhang W, Crisostomo P, *et al*. Endothelial STAT3 plays a critical role in generalized myocardial proinflammatory and proapoptotic signaling. *Am J Physiol Heart Circ Physiol* 2007; 293: H2101-H2108.
68. Knight RA, Scarabelli TM, Stephanou A. STAT transcription in the ischemic heart. *JAKSTAT* 2012; 1: 111-117.
69. Abroun S, Saki N, Ahmadvand M, Asghari F, Salari F, Rahim F. STATs: an old story, yet mesmerizing. *Cell J* 2015; 17: 395-411.
70. Liu S, He Y, Shi J, *et al*. STAT1-avtiviated LINC00961 regulates myocardial infarction by the PI3K/AKT/GSK3β signaling pathway. *J Cell Biochem* 2019; 120: 13226-13236.
71. Nishinakamura H, Minoda Y, Saeki K, *et al*. An RNA-binding protein alphaCP-1 is involved in the STAT3-mediated suppression of NF-kappaB transcriptional activity. *Int Immunol* 2007; 19: 609-619.
72. Verma SK, Krishnamurthy P, Barefield D, *et al*. Interleukin-10 treatment attenuates pressure overload-induced hypertrophic remodeling and improves heart function via signal transducers and activators of transcription 3-dependent inhibition of nuclear factor-κB. *Circulation* 2012; 126: 418-429.
73. Bolli R, Stein AB, Guo Y, *et al*. A murine model of inducible, cardiac-specific deletion of STAT3: its use to determine the role of STAT3 in the upregulation of cardioprotective proteins by ischemic preconditioning. *J Mol Cell Cardiol* 2011; 50: 589-597.
74. Lecour S, Suleman N, Deuchar GA, *et al*. Pharmacological preconditioning with tumor necrosis factor-alpha activates signal transducer and activator of transcription-3 at reperfusion without involving classic prosurvival kinases (Akt and extracellular signal-regulated kinase). *Circulation* 2005; 112: 3911-3818.
75. Boengler K, Hilfiker-Kleiner D, Heusch G, Schulz R. Inhibition of permeability transition pore opening by mitochondrial STAT3 and its role in myocardial ischemia/reperfusion. *Basic Res Cardiol* 2010; 105: 771-785.
76. Miura T, Tanno M. The mPTP and its regulatory proteins: final common targets of signalling pathways for protection against necrosis. *Cardiovasc Res* 2012; 94: 181-189.
77. Hilfiker-Kleiner D, Kaminski K, Podewski E, *et al*. A cathepsin D-cleaved 16 kDa form of prolactin mediates postpartum cardiomyopathy. *Cell* 2007 Feb; 128: 589-600.
78. Jonchere B, Belanger A, Guette C, Barre B, Coqueret O. STAT3 as a new autophagy regulator. *JAKSTAT* 2013; 2: e24353. doi: 10.4161/jkst.24353
79. You L, Wang Z, Li H, *et al*. The role of STAT3 in autophagy. *Autophagy* 2015; 11: 729-739.
80. Chen L, Zhao L, Samanta A, *et al*. STAT3 balances myocyte hypertrophy vis-a-vis autophagy in response to angiotensin II by modulating the AMPKα/mTOR axis. *PLoS One* 2017; 12: e0179835. doi: 10.1371/journal.pone.0179835
81. Szczepanek K, Chen Q, Derecka M, *et al*. Mitochondrial-targeted signal transducer and activator of transcription 3 (STAT3) protects against ischemia-induced changes in the electron transport chain and the generation of reactive oxygen species. *J Biol Chem* 2011; 286: 29610-29620.
82. Ricke-Hoch M, Bultmann I, Stapel B, *et al*. Opposing roles of Akt and STAT3 in the protection of the maternal heart from peripartum stress. *Cardiovasc Res* 2014; 101: 587-596.
83. Nagata T, Yasukawa H, Kyogoku S, *et al*. Cardiac-specific SOCS3 deletion prevents in vivo myocardial ischemia reperfusion injury through sustained activation of cardioprotective signaling molecules. *PLoS One* 2015; 10: e0127942. doi: 10.1371/journal.pone.0127942
84. Kishore R, Verma SK. Roles of STATs signaling in cardiovascular diseases. *JAKSTAT* 2012; 1: 118-124.
85. Kurdi M, Sivakumaran V, Duhe RJ, Aon MA, Paolocci N, Booz GW. Depletion of cellular glutathione modulates LIF-induced JAK1-STAT3 signaling in cardiac myocytes. *Int J Biochem Cell Biol* 2012; 44: 2106-2115.
86. Zgheib C, Kurdi M, Zouein FA, *et al*. Acyloxy nitroso compounds inhibit LIF signaling in endothelial cells and cardiac myocytes: evidence that STAT3 signaling is redox-sensitive. *PLoS One* 2012; 7: e43313. doi: 10.1371/journal.pone.0043313

Received: November 5, 2020
Accepted: December 31, 2020

Author's address: Dr. Ghadeer M. Albadrani, P.O. Box 84428, Riyadh 11671, Saudi Arabia.
E-mail: gmalbadrani@pnu.edu.sa